Robust Spectrum Sensing for Noncircular Signal in Multiantenna Cognitive Receivers

Lei Huang, *Senior Member, IEEE*, Yu-Hang Xiao, and Q. T. Zhang, *Fellow, IEEE*

Abstract—Although noncircular (NC) signals are frequently encountered in wireless communications, their statistical property has not yet been utilized in state-of-the-art methods for spectrum sensing. In this paper, a variant of Hadamard (HDM) ratio test is devised to exploit the NC property of the primary signals for spectrum sensing, which is named the NC-HDM algorithm. As the NC-HDM approach is able to exploit full statistical property of the NC signals and handle deviations from independent and identically distributed (IID) noise, it is superior to the state-of-the-art algorithms in detection accuracy and/or robustness. Moreover, performance analysis is conducted for the NC-HDM approach, including the invariant property, false-alarm probability and detection probability. That is, employing the moment-matching Box's Chi-square approximation, the false-alarm probability can be determined. Since the *exact* moments of the NC-HDM test statistic under the signal-absence hypothesis can be determined and all moments have been matched, the derived false-alarm probability is very accurate, leading to simple and precise computation of the theoretical decision threshold. On the other hand, as the first two *exact* moments of the NC-HDM test statistic under the signal-presence hypothesis can be precisely calculated, the detection probability based on moment-matching Beta approximation is quite accurate. Numerical results are included to demonstrate the superiority of the NC-HDM approach and validate our theoretical calculations.

Index Terms—Beta distribution, generalized likelihood ratio test, multiple antenna, noncircular, spectrum sensing.

I. INTRODUCTION

AS a fundamental element in cognitive radio (CR) [1]–[3], spectrum sensing has received much attention in the literature. Up to now, numerous methodologies have been devised for spectrum sensing, including energy detection (ED), feature detection and correlation-structure detection algorithms. With the known noise variance, it is proved that the ED method [4], [5] is optimal for independent and identically distributed (IID) observations. Nevertheless, its optimality cannot be guaranteed for the situation of unknown noise variance because it is rather sensitive to the noise uncertainty, particularly for the non-IID noise. As a non-blind approach, the feature detector [6]–[8] needs to employ some *a priori* knowledge of the signal or channel to construct its test statistic. Although the feature detection approach is robust against the non-IID noise and provides superior detection performance, it usually suffers from synchronization errors and frequency offsets in practical situations, thereby limiting its applications. Indeed, the presence of primary signals not only changes the energy in the observation data but the correlation structure as well. The correlation structure inherent in the observation covariance matrix leads to the most spread-out eigen-spectrum, providing a good indication for the primary signals. In addition, unlike the ED and feature detection schemes, the eigenvalue-based approach is free of the noise variance and signal features, thereby being a blind detector. As a result, the eigenvalue-based spectrum sensing approaches have received much attention [9]–[14]. As a variant of the generalized likelihood ratio test (GLRT), the spherical test (ST) detector [15] is able to reliably identify the correlated signals embedded in additive IID noise. In fact, the ST detector is equivalent to the eigenvalue arithmetic-to-geometric mean (AGM) algorithm [16]. Nevertheless, it is shown in [17] that, as the locally most powerful invariant test for sphericity, John's detector [18] is superior to the ST detector when the numbers of antennas and samples tend to infinity at the same rate. As a matter of fact, the spectrum sensing algorithms above are developed upon the IID noise assumption and thereby not robust against deviations from the IID noise, which is quite relevant in the real-world applications since the multiantenna cognitive receiver is typically uncalibrated. Even though the receiver can be calibrated, the calibration error makes the thermal noise to be non-ideal IID to some extent, which poses a big challenge for practical spectrum sensing.

Various approaches have been suggested for robust spectrum sensing in the literature, such as the GLRT test [19], independence test [20], Hadamard (HDM) ratio test [21], [22], Gerschgorin disk test [23], locally most powerful invariant test (LMPIT) [24], [25], volume-based test [26], [27] and stochastic learning strategy [28]. Due to its robustness against the non-IID noise and its root in the GLRT paradigm, the HDM approach [29]–[31] has received much attention in the community of spectrum sensing, such as [21], [22]. In the HDM approach, spectrum sensing is cast as the problem of distinguishing between a diagonal matrix and its general Hermitian alternative. A variant of the HDM approach for spectrum sensing has been proposed in [21], where the number of primary users (PUs)

is assumed to be known *a priori* to the receiver. On the other hand, the performance of the HDM algorithm for spectrum sensing has been analyzed in [19], [20]. In fact, as pointed out in [26], although the HDM test is robust against the non-IID noise, its detection performance can be further enhanced.

Note that the HDM test considers the deviation from the IID noise but implicitly utilizes the circularity of the primary signals. However, not all digital modulation schemes produce the circular signals. As a matter of fact, the noncircular (NC) signals are frequently encountered in wireless communication systems, such as the binary phase shift keying (BPSK), offset quaternary phase shift (QPSK), pulse amplitude modulation (PAM), minimum shift keying (GMSK), Gaussian MSK, and baseband orthogonal frequency division multiplexing (OFDM) [32]–[36]. As defined in [37], a complex-valued random vector is noncircular provided that it has a non-zero complementary covariance matrix. In the presence of NC primary signals, the standard HDM test only employs the usual covariance matrix for spectrum sensing but ignores the complementary covariance matrix, thereby being unable to utilize the complete statistical property of the NC primary signals. To achieve the optimal detection performance, the spectrum sensing methodologies rely on not only the usual covariance matrix but also the complementary covariance matrix. Basically, the information in the complementary covariance matrix can be accessed by employing widely linear (WL) or conjugate-linear transformation. The methods for spectrum sensing can considerably improve in detection performance provided that the whole statistical properties of the primary signals can be adopted.

In this paper, we reformulate the HDM test by using the WL transformations and considering the unknown non-IID noises, ending up with an accurate and robust NC-based Hadamard (NC-HDM) ratio test. Moreover, the performance of the NC-HDM approach is analyzed, including the verification of the invariant property as well as derivations of the false-alarm and detection probabilities. In particularly, the false-alarm probability is determined by employing the moment-based Box's approximation. Since the *exact* moments of the NC-HDM test statistic under the signal-absence hypothesis can be obtained and all the moments can be matched, the derived false-alarm probability is very accurate, leading to simple and precise computation of the theoretical decision threshold. On the other hand, as the first two *exact* moments of the NC-HDM test statistic under the signal-presence hypothesis can be precisely calculated, the derived detection probability based on moment-matching Beta approximation is quite accurate. This enables us to precisely evaluate the performance of the NC-HDM approach.

The remainder of the paper is organized as follows. Section II presents the problem formulation, including the noncircularity, signal model as well as HDM test. The NC-HDM algorithm is developed in Section III. Performance analysis of the NC-HDM method is conducted in Section IV. Simulation results are presented in Section V. Finally, conclusions are drawn in Section VI.

Throughout this paper, we use boldface uppercase letter for matrix, boldface lowercase letter for column vector or collection, and lowercase letter for scalar quantity. Superscripts $^{\mathrm{T}}$ and $^{\mathrm{H}}$ represent transpose and conjugate transpose, respectively.

The $E[a]$ and $\hat{a}$ denote the expected value and estimate of a, respectively. The $|\mathbf{A}|$ and $\mathrm{tr}(\mathbf{A})$ are the determinant and trace of $\mathbf{A}$, respectively. The $\mathbf{x} \sim \mathcal{N}(\boldsymbol{\mu}, \mathbf{R})$ means $\mathbf{x}$ follows a complex Gaussian distribution with mean $\boldsymbol{\mu}$ and covariance matrix $\mathbf{R}$, and $\sim$ signifies "distributed as". The $\mathcal{W}_M(N, \mathbf{R})$ and $\mathcal{CW}_M(N, \mathbf{R})$ represent the real and complex Wishart distributions with N degrees of freedom (DOFs) and associated covariance matrix $\mathbf{R}$, respectively. The a_{ij} stands for the (i, j)-th element of $\mathbf{A}$ and $\mathbf{A} \succ \mathbf{B}$ means that $\mathbf{A} - \mathbf{B}$ is a positive definite matrix. The $\mathrm{diag}(\,\cdot\,)$ stands for a diagonal matrix and $\mathbf{I}_M$ represents the $M \times M$ identity matrix.

II. PROBLEM FORMULATION

A. Non-Circularity

For a zero-mean Gaussian random vector $\mathbf{x}$, its usual covariance matrix is defined as $\mathbf{R} = E[\mathbf{x}\mathbf{x}^{\mathrm{H}}]$ and complementary covariance matrix is defined as $\tilde{\mathbf{R}} = E[\mathbf{x}\mathbf{x}^{\mathrm{T}}]$. The random vector $\mathbf{x}$ is circular if $\tilde{\mathbf{R}} = 0$ and noncircular if $\tilde{\mathbf{R}} \neq 0$. For a zero-mean noncircular Gaussian random vector, not only $\mathbf{R}$ but also $\tilde{\mathbf{R}}$ are needed to completely characterize its statistical behavior.

B. Signal Model

Consider a cognitive MIMO network in which a secondary user (SU) with M antennas is attempting to sense the signals emitted by q PUs with a single antenna. The output of the SU, under binary hypotheses, can be written as

$$\mathbf{x} = \begin{cases} \mathbf{n}, & \mathcal{H}_0 \\ \mathbf{Hu} + \mathbf{n}, & \mathcal{H}_1 \end{cases} \tag{1}$$

where $\mathcal{H}_0$ stands for the signal-absence hypothesis, $\mathcal{H}_1$ denotes the signal-presence hypothesis, $\mathbf{H} \in \mathbb{C}^{M \times q}$ corresponds to the MIMO channels between the PUs and SU, which is unknown deterministic during the sensing period. Moreover,

$$\mathbf{x} = [x_1, \dots, x_M]^{\mathrm{T}} \tag{2}$$

$$\mathbf{u} = [u_1, \dots, u_q]^{\mathrm{T}} \tag{3}$$

$$\mathbf{n} = [n_1, \dots, n_M]^{\mathrm{T}} \tag{4}$$

stand for the observation, signal and noise vectors, respectively. It is assumed that $u_i (i = 1, \dots, q)$ is noncircular and Gaussian distributed, i.e., $u_i \sim \mathcal{N}(0, \sigma_{u_i})$ with $\sigma_{u_i} = E[|u_i|^2]$ being the unknown power of u_i and $E[u_i^2] = \kappa_i e^{i \phi_i} \sigma_{u_i}$ with $\iota = \sqrt{-1}$, $\phi_i \in [-\pi, \pi)$ being the noncircularity phase and $\kappa_i \in [0, 1]$ being the noncircularity rate. Moreover, assume that the noise is circular and Gaussian distributed, i.e., $E[n_i^2] = 0$ and $n_i \sim \mathcal{N}(0, \sigma_{n_i})$ $(i = 1, \dots, M)$ where $\sigma_{n_i} = E[|n_i|^2]$ is the unknown noise variance. Note that σ_{n_i} is not necessarily equal to σ_{n_j} for $i \neq j$ in practice, which corresponds to the case of uncalibrated receiver. In addition, the noises are assumed to be statistically independent of each other and also independent of the signals. The spectrum sensing issue at hand is to decide whether the primary signals exist or not from the noisy observations $\mathbf{X} = [\mathbf{x}_1, \cdots, \mathbf{x}_N]$ with N denoting the number of samples.

C. HDM Test

For non-IID noise situations, the observation vector is Gaussian distributed, i.e.,

$$\mathbf{x}|\mathcal{H}_i \sim \mathcal{N}(\mathbf{0}, \mathbf{R}^{(i)}), i = 0, 1 \tag{5}$$

where $\mathbf{R}^{(0)} \triangleq \operatorname{diag}(\sigma_{n_1}, \ldots, \sigma_{n_M})$ and $\mathbf{R}^{(1)} \triangleq (r_{ij})_{M \times M}$ which is non-diagonal and positive definite. According to the GLRT principle, that is, calculating the maximum likelihood (ML) estimates of $\mathbf{R}^{(i)}$ under the binary hypotheses and substituting the so-obtained ML estimates into the likelihood ratio formula, the HDM test is

$$\xi_{\text{HDM}} = \frac{|\mathbf{S}|}{\prod_{i=1}^{M} s_{ii}} \underset{\mathcal{H}_1}{\overset{\mathcal{H}_0}{\gtrless}} \gamma_{\text{HDM}} \qquad (6)$$

where $\mathbf{S} = (1/N)\mathbf{X}\mathbf{X}^{\text{H}}$, $s_{ii}(i = 1, \ldots, M)$ is the diagonal element of $\mathbf{S}$ and γ_{HDM} is the decision threshold of the HDM scheme. The HDM test was first proposed in [29] for multivariate statistical analysis, then reformulated for Gaussian signal detection in the community of array processing [30], [31] and recently exploited for spectrum sensing [19]–[21]. Although the Hadamard ratio approach is robust against the deviation from the IID noise, it only utilizes the usual covariance matrix for detecting the presence of primary signals, ignoring the complementary covariance matrix. As a result, the HDM approach is unable to employ the whole statistical characterization of complex-valued data for spectrum sensing. This eventually leads to the sub-optimal detection performance in the NC primary signal scenarios.

III. PROPOSED NC-HDM TEST

It is desired to develop a robust detection approach for spectrum sensing, which is able to employ the complete statistical characterization of the complex-valued observation data. For the NC Gaussian signals, not only the usual covariance matrix but also the complementary covariance matrix are required to completely characterize the statistical behavior of the complex-valued data. To guarantee the robustness and accuracy in spectrum sensing, the NC-HDM detection algorithm is devised in this subsection. In particular, let $\underline{\mathbf{x}} = [\mathbf{x}^{\text{T}}, \mathbf{x}^{\text{H}}]^{\text{T}}$ be the augmented observation vector. It follows from [36] that the probability density function (PDF) of $\underline{\mathbf{x}}$ is

$$f(\underline{\mathbf{x}}) = \frac{1}{\pi^N |\underline{\mathbf{R}}|^{1/2}} \exp\left\{-\frac{1}{2}\underline{\mathbf{x}}^{\text{H}}\underline{\mathbf{R}}^{-1}\underline{\mathbf{x}}\right\} \qquad (7)$$

where $\underline{\mathbf{R}}$ is the augmented covariance matrix, given as

$$\underline{\mathbf{R}} = E[\underline{\mathbf{x}}\underline{\mathbf{x}}^{\text{H}}] = \begin{bmatrix} \mathbf{R} & \tilde{\mathbf{R}} \\ \tilde{\mathbf{R}}^* & \mathbf{R}^* \end{bmatrix} \in \mathbb{C}^{2M \times 2M}. \qquad (8)$$

If $\tilde{\mathbf{R}} = \mathbf{0}$, $\mathbf{x}$ is circular; otherwise, it is noncircular. For $\tilde{\mathbf{R}} \neq \mathbf{0}$, the primary signals can be the BPSK, offset QPSK and baseband OFDM which are of the NC property. The sensing problem can be formulated as the following hypothesis test:

$$\mathcal{H}_0 : \tilde{\mathbf{R}} = \mathbf{0}, \mathbf{R} = \operatorname{diag}(\sigma_{n_1}, \ldots, \sigma_{n_M}) \qquad (9)$$
$$\mathcal{H}_1 : \tilde{\mathbf{R}} \neq \mathbf{0}, \mathbf{R} \neq \operatorname{diag}(\sigma_{n_1}, \ldots, \sigma_{n_M}). \qquad (10)$$

It is easy to obtain the likelihood function under hypothesis $\mathcal{H}_i(i = 1, 2)$ as

$$\mathcal{L}(\mathbf{X}|\mathcal{H}_i) = |\underline{\mathbf{R}}^{(i)}|^{-\frac{N}{2}} \exp\left(-\frac{1}{2}\operatorname{tr}\left([\underline{\mathbf{R}}^{(i)}]^{-1}\underline{\mathbf{W}}\right)\right) \qquad (11)$$

TABLE I
PROPOSED NC-HDM ALGORITHM

Step 1: Compute the augmented SCM by $\underline{\mathbf{W}} = \sum_{t=1}^{N} \underline{\mathbf{x}}_t \underline{\mathbf{x}}_t^{\text{H}}$.
Step 2: Construct the test statistic

$$\xi_{\text{NC-HDM}} = \frac{|\underline{\mathbf{W}}|^{\frac{1}{2}}}{\prod_{i=1}^{M} w_{ii}}.$$

Step 3: Determine the presence or not of the primary signals by comparing $\xi_{\text{NC-HDM}}$ with the predetermined threshold $\gamma_{\text{NC-HDM}}$. If $\xi_{\text{NC-HDM}} > \gamma_{\text{NC-HDM}}$, the signal is absent; otherwise, the signal is present.

where the constant term has been dropped for simplicity and $\underline{\mathbf{W}}$ is the augmented sample covariance matrix (SCM), computed as

$$\underline{\mathbf{W}} = \sum_{t=1}^{N} \underline{\mathbf{x}}_t \underline{\mathbf{x}}_t^{\text{H}} = \begin{bmatrix} \mathbf{W} & \tilde{\mathbf{W}} \\ \tilde{\mathbf{W}}^* & \mathbf{W}^* \end{bmatrix} = (w_{ij})_{2M \times 2M}. \qquad (12)$$

According to the GLRT principle, the test statistic can be expressed as

$$T = \frac{\sup_{\underline{\mathbf{R}}^{(0)}} \mathcal{L}(\mathbf{X}|\mathcal{H}_0)}{\sup_{\underline{\mathbf{R}}^{(1)}} \mathcal{L}(\mathbf{X}|\mathcal{H}_1)}. \qquad (13)$$

By setting the derivative of logarithm of (13) with respect to $\underline{\mathbf{R}}^{(i)}$ to zero, we obtain that the ML estimates of $\underline{\mathbf{R}}^{(1)}$ is $\hat{\underline{\mathbf{R}}}^{(1)} = (1/N)\underline{\mathbf{W}}$, and the ML estimate of $\underline{\mathbf{R}}^{(0)}$ is $\hat{\underline{\mathbf{R}}}^{(0)} = (1/N)\operatorname{diag}(w_{11}, \ldots, w_{MM}, w_{11}, \ldots, w_{MM})$. Substituting the ML estimates into (13), we obtain the GLRT test statistic as

$$\xi_{\text{NC-HDM}} \triangleq T^{\frac{1}{N}} = \frac{|\underline{\mathbf{W}}|^{\frac{1}{2}}}{\prod_{i=1}^{M} w_{ii}}. \qquad (14)$$

Let $\gamma_{\text{NC-HDM}}$ be the decision threshold of the NC-HDM method. The null hypothesis $\mathcal{H}_0$ is rejected if $\xi_{\text{NC-HDM}}$ is smaller than $\gamma_{\text{NC-HDM}}$; otherwise, the alternative hypothesis $\mathcal{H}_1$ is rejected. That is

$$\xi_{\text{NC-HDM}} \underset{\mathcal{H}_1}{\overset{\mathcal{H}_0}{\gtrless}} \gamma_{\text{NC-HDM}}. \qquad (15)$$

The NC-HDM sensing algorithm is summarized in Table I.

IV. PERFORMANCE ANALYSIS

In this section, the performance analysis is conducted for the proposed NC-HMD approach. In particular, the invariant property of the NC-HMD test is first proved in Section IV.A. Then, the accurate analytical expression is derived for computing the false-alarm probability by utilizing the moment-matching Box's Chi-square approximation in Section IV.B. Finally, the theoretical detection probability of the NC-HDM test is determined by employing the moment-matching Beta approximation in Section IV.C.

A. Invariant Property

Invariance is an important property for the hypothesis test. It is easy to verify that the proposed NC-HDM algorithm is

of the invariant property. In particular, for a group of invariant transformations:

$$\mathcal{Z} = \{z : \mathbf{x} \rightarrow z(\mathbf{x}) = \mathbf{Z}\mathbf{x}, \mathbf{Z} = \mathbf{I}_2 \otimes \mathbf{P}, \mathbf{P} \in \mathbb{D}\} \quad (16)$$

where $\mathbb{D}$ is a group of diagonal positive-definite matrices of dimension M and $\mathbf{Z} = \text{diag}\{p_1, \dots, p_M, p_1, \dots, p_M\}$ with p_i being non-zero real-valued number, we easily have

$$\breve{\mathbf{x}} = \mathbf{Z}\underline{\mathbf{x}} \quad (17)$$
$$\breve{\mathbf{W}} = \mathbf{Z}\underline{\mathbf{W}}\mathbf{Z}^{\mathrm{H}}. \quad (18)$$

It follows from (14) that

$$\xi_{\text{NC-HDM}}\{\breve{\mathbf{W}}\} = \frac{\left|\breve{\mathbf{W}}\right|^{\frac{1}{2}}}{\prod_{i=1}^{M} \breve{w}_{ii}} = \frac{|\mathbf{Z}|^{\frac{1}{2}} \times |\underline{\mathbf{W}}|^{\frac{1}{2}} \times |\mathbf{Z}^{\mathrm{H}}|^{\frac{1}{2}}}{\prod_{i=1}^{M} w_{ii} \times p_i^2} \quad (19)$$

$$= \xi_{\text{NC-HDM}}\{\underline{\mathbf{W}}\} \quad (20)$$

which indicates that the NC-HDM test is invariant.

B. False-Alarm Probability

In this subsection, we will derive accurate false-alarm probability by means of the Box's approximation [38], [39], enabling us to determine accurate theoretical decision threshold for the NC-HDM approach. To this end, we first need to compute the moments of the test statistic.

Under $\mathcal{H}_0$, it follows from [37] that the PDF of $\underline{\mathbf{W}}$ can be derived from that of the Wishart distribution, which is given as

$$p(\underline{\mathbf{W}}) = \frac{|\underline{\mathbf{W}}|^{\frac{N-1}{2}-M} \exp\left\{-\frac{1}{2}\text{tr}[\underline{\mathbf{R}}^{-1}\underline{\mathbf{W}}]\right\}}{2^{M(N-2M-1)}\Gamma_{2M}\left(\frac{N}{2}\right)|\underline{\mathbf{R}}|^{\frac{N}{2}}} \quad (21)$$

where

$$\Gamma_{2M}\left(\frac{N}{2}\right) = \pi^{M(2M-1)/2} \prod_{i=1}^{2M} \Gamma\left(\frac{N-i+1}{2}\right). \quad (22)$$

with $\Gamma(\,\cdot\,)$ being the complete Gamma function. Given the PDF of $\underline{\mathbf{W}}$ in (21), the k-th moment of $\xi_{\text{NC-HDM}}$ is computed as

(23), given at the bottom of the page. Here, w'_{ii} is the i-th diagonal element of $\underline{\mathbf{W}}'$ which has the same distribution as $\underline{\mathbf{W}}$ but with DOFs of $N + k$. On the other hand, note that $2w'_{ii}/\sigma_{n_i}$ follows a Chi-square distribution with DOFs of $2(N + k)$. Using the moment expression for Chi-square distribution, we obtain the $(-k)$-th moment of $\prod_{i=1}^{M} w'_{ii}$ as

$$E\left[\left(\prod_{i=1}^{M} w'_{ii}\right)^{-k}\right] = \left(\prod_{i=1}^{M} \sigma_{n_i}\right)^{-k} \left[\frac{\Gamma(N)}{\Gamma(N+k)}\right]^{M}. \quad (24)$$

Substituting (24) into (23) and recalling $|\underline{\mathbf{R}}|^{1/2} = \prod_{i=1}^{M} \sigma_{n_i}$ under $\mathcal{H}_0$, we obtain the k-th moment of $\xi_{\text{NC-HDM}}$ as

$$E[\xi_{\text{NC-HDM}}^k] = \frac{2^{Mk}\Gamma_{2M}\left(\frac{N+k}{2}\right)}{\Gamma_{2M}\left(\frac{N}{2}\right)} \left[\frac{\Gamma(N)}{\Gamma(N+k)}\right]^{M},$$
$$k = 0, 1, \dots \quad (25)$$

Having determined the moments of $\xi_{\text{NC-DHM}}$ above, we can utilize the Box's approximation to derive the false-alarm probability. To proceed, the following results [38], [39] are needed.

Lemma 1: If a random variable $\phi \in [0, 1]$ has the k-th moment, expressed as

$$E[\phi^k] = C_0 \left(\frac{\prod_{j=1}^{b} y_j^{y_j}}{\prod_{i=1}^{a} x_i^{x_i}}\right)^k \frac{\prod_{i=1}^{a}\Gamma[x_i(1+k)+\xi_i]}{\prod_{j=1}^{b}\Gamma[y_j(1+k)+\eta_j]},$$
$$k = 0, 1, \dots \quad (26)$$

in which a and b are integers, $\sum_{i=1}^{a} x_i = \sum_{j=1}^{b} y_j$ and C_0 is a constant such that $E[\phi] = 1$, then the cumulative distribution function (CDF) of $-2\rho \ln \phi$ can be determined as

$$P\{-2\rho \ln \phi \leq \gamma\} = P\left\{\chi_f^2 \leq \gamma\right\} + \omega \left[P\left\{\chi_{f+4}^2 \leq \gamma\right\}\right.$$
$$\left. -P\left\{\chi_f^2 \leq \gamma\right\}\right] + \sum_{k=1}^{a}\mathcal{O}\left(x_k^{-3}\right) + \sum_{j=1}^{b}\mathcal{O}\left(y_j^{-3}\right) \quad (27)$$

where

$$f = -2\left\{\sum_{i=1}^{a}\xi_i - \sum_{j=1}^{b}\eta_j - \frac{1}{2}(a-b)\right\} \quad (28a)$$

$$E\left[\xi_{\text{NC-HDM}}^k\right] = \int_{\underline{\mathbf{W}}>0} \frac{|\underline{\mathbf{W}}|^{\frac{N+k-1}{2}-M} \exp\left\{-\frac{1}{2}\text{tr}\left[\underline{\mathbf{R}}^{-1}\underline{\mathbf{W}}\right]\right\}}{2^{M(N-2M-1)}\Gamma_{2M}\left(\frac{N}{2}\right)|\underline{\mathbf{R}}|^{\frac{N}{2}} \prod_{i=1}^{M} w_{ii}^k} d\underline{\mathbf{W}}$$

$$= \frac{2^{Mk}|\underline{\mathbf{R}}|^{\frac{k}{2}}\Gamma_{2M}\left(\frac{N+k}{2}\right)}{\Gamma_{2M}\left(\frac{N}{2}\right)}$$

$$\times \int_{\underline{\mathbf{W}}'>0} \frac{|\underline{\mathbf{W}}'|^{\frac{N+k-1}{2}-M} \exp\left\{-\frac{1}{2}\text{tr}\left[\underline{\mathbf{R}}^{-1}\underline{\mathbf{W}}'\right]\right\}}{2^{M(N+k-2M-1)}\Gamma_{2M}\left(\frac{N+k}{2}\right)|\underline{\mathbf{R}}|^{\frac{N+k}{2}} \prod_{i=1}^{M} w_{ii}'^k} d\underline{\mathbf{W}}'$$

$$= \frac{2^{Mk}|\underline{\mathbf{R}}|^{\frac{k}{2}}\Gamma_{2M}\left(\frac{N+k}{2}\right)}{\Gamma_{2M}\left(\frac{N}{2}\right)} E\left[\left(\prod_{i=1}^{M} w'_{ii}\right)^{-k}\right] \quad (23)$$

$$\rho = 1 - \frac{1}{f}\left(\sum_{i=1}^{a}\frac{\xi_i^2 - \xi_i + \frac{1}{6}}{x_i} - \sum_{j=1}^{b}\frac{\eta_j^2 - \eta_j + \frac{1}{6}}{y_j}\right) \quad (28b)$$

$$\omega = -\frac{1}{6}\left\{\sum_{i=1}^{a}\frac{B(\mu_i + \xi_i)}{(\rho x_i)^2} - \sum_{j=1}^{b}\frac{B(\nu_j + \eta_j)}{(\rho y_j)^2}\right\} \quad (28c)$$

with $B(\ell) = \ell^3 - 1.5\ell^2 + 0.5\ell$ being the Bernoulli polynomial with DOFs of 3 and order one, and

$$\mu_i = (1 - \rho)x_i \quad (29)$$
$$\nu_j = (1 - \rho)y_j. \quad (30)$$

We are now at a position to match the k-th moment of ϕ to that of $\xi_{\text{NC-HDM}}$ for arbitrary $k = 0, 1, \ldots$ but within the same support $[0, 1]$. Recalling that $\underline{\mathbf{W}}$ is non-negative definite, we have $|\underline{\mathbf{W}}| \geq \mathbf{0}$, leading to $\xi_{\text{NC-HDM}} \geq 0$. On the other hand, using the inequality of $|\underline{\mathbf{W}}| \leq \prod_{i=1}^{M} w_{ii}^2$ in ([40], p. 477), we have $\xi_{\text{NC-HDM}} \leq 1$. Thus, we obtain $\xi_{\text{NC-HDM}} \in [0, 1]$. It follows from (25) that the k-th moment of $\xi_{\text{NC-HDM}}^N \in [0, 1]$ is

$$E\left[\xi_{\text{NC-HDM}}^{Nk}\right] = \frac{2^{MNk}\Gamma_{2M}\left(\frac{N+Nk}{2}\right)}{\Gamma_{2M}\left(\frac{N}{2}\right)}\left[\frac{\Gamma(N)}{\Gamma(N+Nk)}\right]^M$$
$$= C(M, N)\frac{2^{MNk}\prod_{i=1}^{2M}\Gamma\left(\frac{N(1+k)-i+1}{2}\right)}{[\Gamma(N(1+k))]^M}$$
$$(31)$$

where $C(M, N) = [\Gamma(N)]^M / \prod_{i=1}^{2M}\Gamma(\frac{N-i+1}{2})$ which is independent of k. By matching the k-th moment of ϕ to that of $\xi_{\text{NC-HDM}}^N$, it follows from (26) and (31) that

$$a = 2M \quad (32a)$$
$$b = M \quad (32b)$$
$$x_i = \frac{N}{2} \quad (32c)$$
$$y_j = N \quad (32d)$$
$$\xi_i = \frac{1-i}{2} \quad (32e)$$
$$\eta_j = 0. \quad (32f)$$

Substituting (32) into (28) yields

$$f = 2M^2 \quad (33a)$$

$$\rho = 1 - \frac{1}{4M^2 N}\left(\sum_{i=1}^{2M}i^2 - M\right) \quad (33b)$$

$$\omega = \frac{MB[(1-\rho)N]}{6\rho^2 N^2} - \frac{2}{3\rho^2 N^2}\sum_{i=1}^{2M}B\left[\frac{(1-\rho)N - i + 1}{2}\right]. (33c)$$

Setting $\xi_{\text{NC-HDM}}^N = \phi$ and ignoring the terms of $\mathcal{O}(N^{-3})$, it follows from (27) that the CDF is asymptotically given as

$$F_\xi(\gamma) = 1 - P\left(\chi_f^2 \leq -2\rho N \ln \gamma\right)$$
$$-\omega\left[P\left(\chi_{f+4}^2 \leq -2\rho N \ln \gamma\right) - P\left(\chi_f^2 \leq -2\rho N \ln \gamma\right)\right]. \quad (34)$$

Thus, given a false-alarm probability P_{fa}, the decision threshold can be obtained by numerically inverting $F_\xi(\gamma)$. That is,

$$\gamma_{\text{NC-HDM}} = F_\xi^{-1}(P_{\text{fa}}). \quad (35)$$

C. Detection Probability

In Section VI-B, the false-alarm probability is computed by matching all moments of $\xi_{\text{NC-HDM}}^N$ under $\mathcal{H}_0$, i.e., $E[\xi_{\text{NC-HDM}}^{Nk}] (k = 0, 1, \ldots)$, to those of ϕ whose fluctuation can be asymptotically determined by the Chi-square distribution. Nevertheless, it is very difficult to determine all the moments of $\xi_{\text{NC-HDM}}^N$ under $\mathcal{H}_1$. Indeed, it is shown in [12], [20], [41], [42] that, by computing the first two moments of the test statistic and utilizing the moment-matching Beta approximation, the fluctuations of some well known test statistics, such as the ST, John's and HDM, can be accurately determined. This is because these test statistics have the same support as the Beta distribution, i.e., $\xi \in [0, 1]$. Note that $\xi_{\text{NC-HDM}}^N$ under $\mathcal{H}_1$ also has the support $[0, 1]$. On the other hand, since two parameters are sufficient to completely determine the Beta distribution, only the first two moments of the test statistics are involved. This motivates us to derive the detection probability of the NC-HDM approach by matching the first two moments of $\xi_{\text{NC-HDM}}^N$ to those of the Beta distribution.

Note that the k-th moment of $\xi_{\text{NC-HDM}}^N$ under $\mathcal{H}_1$ has the same expression as (23). Since only two moments are needed for the moment-matching Beta approximation, the first two moments of $\prod_{i=1}^{M} w_{ii}'$ will be considered. It follows from (23) that

$$\mathcal{M}_{-1} \triangleq E\left[\xi_{\text{NC-HDM}}^{-1}\right] = \frac{2^{-M}|\underline{\mathbf{R}}|^{-\frac{1}{2}}\Gamma_{2M}\left(\frac{N-1}{2}\right)}{\Gamma_{2M}\left(\frac{N}{2}\right)}\mathcal{T}_1$$
$$(36)$$

$$\mathcal{M}_{-2} \triangleq E\left[\xi_{\text{NC-HDM}}^{-2}\right] = \frac{2^{-2M}|\underline{\mathbf{R}}|^{-1}\Gamma_{2M}\left(\frac{N-2}{2}\right)}{\Gamma_{2M}\left(\frac{N}{2}\right)}\mathcal{T}_2 \quad (37)$$

with

$$\mathcal{T}_1 = E\left[\prod_{i=1}^{M}w'_{ii}\right] \quad (38a)$$

$$\mathcal{T}_2 = E\left[\prod_{i=1}^{M}w'^2_{ii}\right] \quad (38b)$$

We are now at a position to calculate $\mathcal{T}_1$ and $\mathcal{T}_2$. In order to do so, several existing schemes can be applied. One possible scheme is to adopt the asymptotic non-central Chi-square distribution of w'_{ii} to approximately compute the first two moments of $\prod_{i=1}^{M} w'^2_{ii}$, analogous to the approach in [19]. However, such a scheme cannot provide sufficient accuracy for moment calculation at small samples because the term $\mathcal{O}(1/N)$ needs to be ignored. This eventually leads to poor approximation for the Beta distribution. Another possible scheme is to compute the first and second exact moments by means of the approach provided in [13]. Nevertheless, recall that w'_{ii} is the i-th diagonal element of the WL expression $\underline{\mathbf{W}}'$ with DOFs of $N + k$, whose fluctuation is very difficult to determine. To circumvent this problem, similar to [43], we transform $\underline{\mathbf{W}}'$ into a real-valued matrix and then determine its fluctuation. In particular, for the complex-valued observation $\mathbf{x} = \mathbf{x}_R + \imath\mathbf{x}_I$ in which $\mathbf{x}_R$ and $\mathbf{x}_I$ are the real and imaginary parts of $\mathbf{x}$, respectively, its corresponding real-valued observation is $\check{\mathbf{x}} = [\mathbf{x}_R^{\mathrm{T}}, \mathbf{x}_I^{\mathrm{T}}]^{\mathrm{T}}$ with the SCM of

$$\mathbf{G} = \check{\mathbf{X}}\check{\mathbf{X}}^{\mathrm{T}} = \begin{pmatrix} \mathbf{G}_{RR} & \mathbf{G}_{RI} \\ \mathbf{G}_{IR} & \mathbf{G}_{II} \end{pmatrix} \quad (39)$$

where $\check{\mathbf{X}} = [\check{\mathbf{x}}_1, \ldots, \check{\mathbf{x}}_N]$. As a result, the WL expression can also be given by

$$\underline{\mathbf{W}}' = \mathbf{G}_{RR} + \mathbf{G}_{II} + \imath(\mathbf{G}_{IR} - \mathbf{G}_{RI}). \tag{40}$$

This implies that $\mathcal{T}_1$ and $\mathcal{T}_2$ can be determined by using the real-valued covariance matrix $\mathbf{G}$.

Proposition 1: For any number of antennas M and number of samples N, $\mathcal{T}_1$ and $\mathcal{T}_2$ defined in (38) are computed as

$$\mathcal{T}_1 = \sum_{\ell_1=0}^{1} \sum_{\ell_2=0}^{1} \cdots \sum_{\ell_M=0}^{1} \left\{ \frac{1}{\imath^M} \sum_{\boldsymbol{\pi} \in \mathcal{S}_M} \left[\prod_{m=1}^{p^{(\boldsymbol{\pi})}} (N + 2m - 1) \right] \right.$$
$$\left. \times \left(-\frac{1}{2} \right)^{p^{(\boldsymbol{\pi})}} \prod_{m=1}^{p^{(\boldsymbol{\pi})}} \frac{\partial^{\jmath} |\mathbf{A}_{cc}|}{\partial \pi_{m1} \cdots \partial \pi_{m\jmath}} \bigg|_{\mathbf{D}_{cc}=\mathbf{0}} \right\} \tag{41}$$

$$\mathcal{T}_2 = \sum_{\ell_1=0}^{1} \sum_{\ell_2=0}^{1} \cdots \sum_{\ell_{2M}=0}^{1} \left\{ \frac{1}{\imath^{2M}} \sum_{\boldsymbol{\pi} \in \mathcal{S}_{2M}} \left[\prod_{m=1}^{p^{(\boldsymbol{\pi})}} (N + 2m) \right] \right.$$
$$\left. \times \left(-\frac{1}{2} \right)^{p^{(\boldsymbol{\pi})}} \prod_{m=1}^{p^{(\boldsymbol{\pi})}} \frac{\partial^{\jmath} |\mathbf{A}_{2M}|}{\partial \pi_{m1} \cdots \partial \pi_{m\jmath}} \bigg|_{\mathbf{D}_{2M}=\mathbf{0}} \right\} \tag{42}$$

where $\mathcal{S}_M$ consists of all the partitions of the M-element set $\{t_{i_1}, \ldots, t_{i_M}\}$ with the number of partitions being the Bell number [44] and the index satisfying $i_m = m + \ell_m M (m = 1, \ldots, M)$, $\mathcal{S}_{2M}$ is composed by all the partitions of the $2M$-element set $\{t_{j_1}, \ldots, t_{j_{2M}}\}$ with index satisfying $j_1 = 1 + \ell_1 M, j_2 = 1 + \ell_2 M, j_3 = 2 + \ell_3 M, j_4 = 2 + \ell_4 M, \ldots, j_{2M-1} = M + \ell_{2M-1} M, j_{2M} = M + \ell_{2M} M$. Moreover, $\boldsymbol{\pi}$ in (41) denotes a partition of $\{t_{i_1}, \ldots, t_{i_M}\}$ which is defined as a family of nonempty, pairwise disjoint subsets of $\{t_{i_1}, \ldots, t_{i_M}\}$ whose union is $\{t_{i_1}, \ldots, t_{i_M}\}^1$, $p^{(\boldsymbol{\pi})}$ is the number of subsets in $\boldsymbol{\pi}$, $\boldsymbol{\pi}_m$ is the m-th subset of $\boldsymbol{\pi}$, $\jmath$ is the number of elements in $\boldsymbol{\pi}_m$ and π_{mj} is the j-th entry of $\boldsymbol{\pi}_m$. These definitions are also applicable to (42). Furthermore,

$$|\mathbf{A}_{cc}| = |\mathbf{I}_M - \imath 2 \mathbf{D}_{cc} \boldsymbol{\Sigma}_{cc}| \tag{43}$$

$$|\mathbf{A}_{2M}| = |\mathbf{I}_{2M} - \imath 2 \mathbf{D}_{2M} \boldsymbol{\Sigma}| \tag{44}$$

where $\mathbf{D}_{cc} = \mathrm{diag}(t_{i_1}, \ldots, t_{i_M})$, $\mathbf{D}_{2M} = \mathrm{diag}(t_1, \ldots, t_{2M})$, $\boldsymbol{\Sigma} = E[\check{\mathbf{x}}\check{\mathbf{x}}^T]$ and $\boldsymbol{\Sigma}_{cc}$ is the submatrix of $\boldsymbol{\Sigma}$ with index $\mathbf{c} = \{i_1, \ldots, i_M\}$. Additionally, the partial derivatives of $|\mathbf{A}_{cc}|$ and $|\mathbf{A}|$ with respect to π_{mj} are provided in (62) and (68), respectively.

Proof: The proof is provided in Appendix A. ∎

Let $G_\xi(y)$ be the CDF of $\xi_{\mathrm{NC-HDM}}$ under $\mathcal{H}_1$, which is determined as follows. For any numbers of antennas and samples, i.e., M and N, the moment-matching Beta approximation to the CDF of $\xi_{\mathrm{NC-HDM}}$ under $\mathcal{H}_1$ is

$$G(y) \approx \frac{B_y(\alpha, \beta)}{B(\alpha, \beta)}, y \in [0, 1] \tag{45}$$

where

$$B(\alpha, \beta) = \frac{\Gamma(\alpha)\Gamma(\beta)}{\Gamma(\alpha + \beta)} \tag{46}$$

¹For more details about the partition of a finite nonempty set, the interested reader is referred to [44].

$$B_y(\alpha, \beta) = \int_0^y z^{\alpha-1}(1-z)^{\beta-1} dz \tag{47}$$

are the complete and incomplete Beta functions, respectively, and

$$\alpha = \left(\mathcal{M}_{-1} - \frac{2\mathcal{M}_{-2}}{\mathcal{M}_{-1}} + 1 \right) \left(\mathcal{M}_{-1} - \frac{\mathcal{M}_{-2}}{\mathcal{M}_{-1}} \right) \tag{48a}$$

$$\beta = (1 - \mathcal{M}_{-1})(1 - \alpha). \tag{48b}$$

Thus, it follows from (15) that the detection probability is computed as

$$P_{\mathrm{d}}(\gamma) \triangleq \mathrm{Prob}(\xi < \gamma | \mathcal{H}_1) = G(\gamma). \tag{49}$$

Given a false-alarm level P_{fa}, the theoretical decision threshold is determined by (35). On the other hand, with the so-obtained threshold, the corresponding detection probability is computed by (49). The mapping between the false-alarm probability and detection probability yields the ROC. Hence, the analytical ROC formula for the NC-HDM test is attained as

$$P_{\mathrm{d}} = G(F^{-1}(P_{\mathrm{fa}})). \tag{50}$$

Remark: It is worth pointing out that the number of partitions of the M-element set $\{t_{i_1}, \ldots, t_{i_M}\}$ is the Bell number [44], which considerably increases as M becomes large. As a result, the calculation of the detection probability in (49) is quite computationally intensive particularly when M is large. However, as pointed out in [13], the number of antennas in the SU is typically small in practice, say, M varies from 2 up to 8 due to physical constraints of the device size. On the other hand, recall that the theoretical detection probability is only used to predict the behavior of the NC-HDM test provided that $\underline{\mathbf{R}}$ or $\boldsymbol{\Sigma}$ are given. Note that the relationship between $\underline{\mathbf{R}}$ and $\boldsymbol{\Sigma}$ is same as that between $\underline{\mathbf{W}}'$ and $\mathbf{G}$ in (39) and (40). That is to say, the theoretical detection probability is not used for spectrum sensing and thereby can be computed off-line. Hence, the analytical expression for the detection probability is tractable in the practical spectrum sensing situations.

V. NUMERICAL RESULTS

Simulation results are presented to validate the analytical computations of the false-alarm and detection probabilities, and then illustrate the superiority of the devised NC-HDM approach over the state-of-the-art detection algorithms.

A. Accuracy of Theoretical False-Alarm and Detection Probabilities

The approximate analytical formulae for the false-alarm probability and detection probability are numerically evaluated in this subsection. For the purpose of comparison, the empirical false-alarm and detection probabilities determined by 10^5 Monte Carlo simulation trials are presented as well. In the simulation results, we use "analytical" to stand for the derived analytical false-alarm probability and the "simulation" to represent the empirical false-alarm probability. We first study the accuracy of the approximate false-alarm probability. Fig. 1 plots the false-alarm probability versus decision threshold for
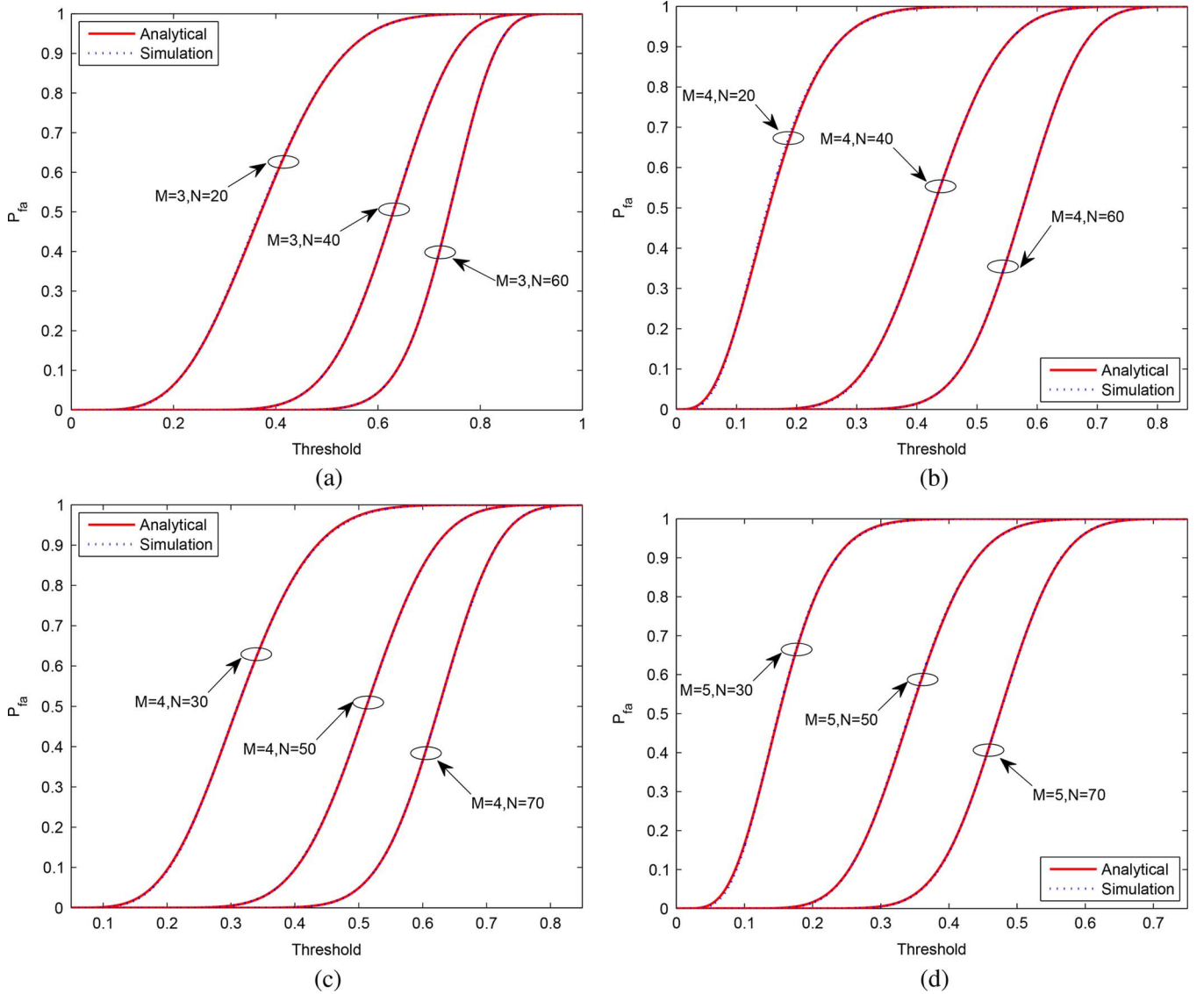
Fig. 1. False-alarm probability versus threshold for various parameter settings. (a) $M = 3$, $N = [20, 40, 60]$ and IID noise. (b) $M = 4$, $N = [20, 40, 60]$ and IID noise. (c) $M = 4$, $N = [30, 50, 70]$ and non-IID noise. (d) $M = 5$, $N = [30, 50, 70]$ and non-IID noise.

various parameter settings. It is seen in Fig. 1 that the asymptotic approximate false-alarm probability is very accurate in terms of fitting the empirical curves. Analogous to [12], [13], to quantitatively demonstrate the accuracy, we employ the Cramér-von Mises criterion [41] to calculate the errors of the derived asymptotic approximation with respect to the exact distribution obtained from the simulations. That is,

$$\text{Error} = \frac{1}{J} \sum_{i=1}^{J} \left| F(y_i) - \hat{F}(y_i) \right|^2 \tag{51}$$

where $F(y_i)$ is the false-alarm probability determined by simulation, $\hat{F}(y_i)$ is its estimate obtained by our derived approximate formula and $J = 10^5$ within the support $[c_1, c_2]$ with $c_1, c_2 \in [0, 1]$ and $c_1 < c_2$. The errors between the analytical and simulated false-alarm probabilities are equal to $[0.20, 0.044, 0.01] \times 10^{-5}$ in Fig. 1(a), $[0.94, 0.09, 0.02] \times 10^{-5}$ in Fig. 1(b), $[0.14, 0.06, 0.039] \times 10^{-5}$ in Fig. 1(c) and $[0.37, 0.18, 0.05] \times 10^{-5}$ in Fig. 1(d). In a word, the error is

around 10^{-5} for $N = 20$ and becomes much smaller than 10^{-5} when the number of samples is larger than 60 no matter the noise is IID or non-IID.

Let us now examine the accuracy of the detection probability for the proposed Beta approximation. The simulation results for the analytical and simulated detection probabilities are depicted in Fig. 2 for various parameter settings. More specifically, we consider the situation of $M = 3$, $N = [40, 80, 160]$, SNR $= 0$ dB for a single primary signal in Rayleigh fading channel in Fig. 2(a), the condition of $M = 3$, $N = [40, 80, 160]$, SNR $= [-0.8, -3.5, -5.2]$ dB for three primary signals in Rayleigh fading channel in Fig. 2(b), the scenario of $M = 4$, $N = [40, 80, 160]$, SNR $= [-0.8, -3.5, -5.2]$ dB for three primary signals in Rayleigh fading channel in Fig. 2(c), and the case of $M = 5$, $N = [40, 120, 200]$, SNR $= [-1.3 - 4.2]$ dB for two primary signals in Rayleigh fading channel in Fig. 2(d). In the meanwhile, the IID and non-IID noises are considered as well. In the Rayleigh fading channel, the entries of $\mathbf{H} = [\mathbf{h}_1, \ldots, \mathbf{h}_q]$ are independently drawn from a standard complex
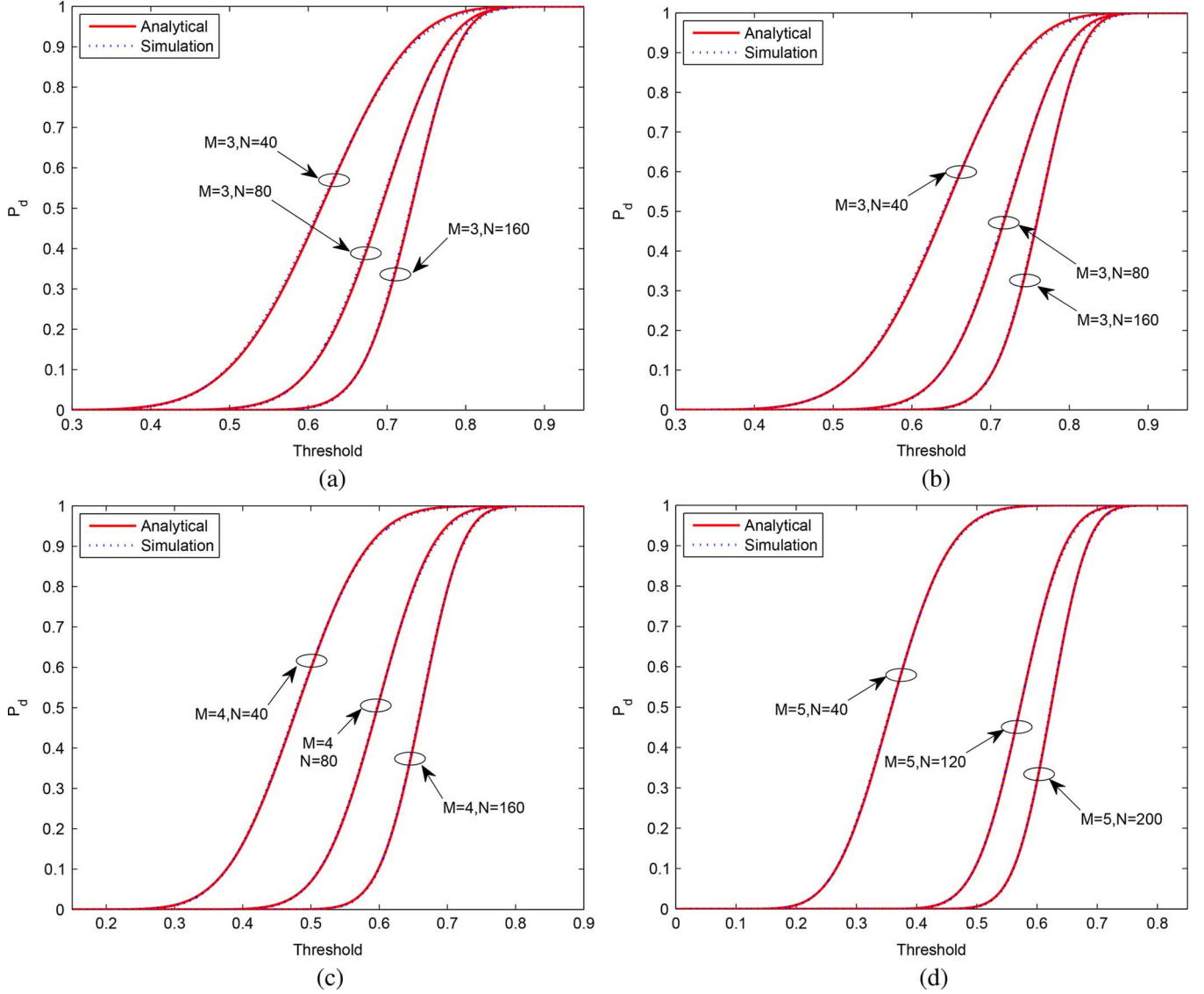
Fig. 2. Detection probability versus threshold for various parameter settings. (a) $M = 3$, $N = [40, 80, 160]$, SNR $= 0$ dB and IID noise. (b) $M = 3$, $N = [40, 80, 160]$, SNR $= [-0.8, -3.5, -5.2]$ dB and non-IID noise. (c) $M = 4$, $N = [40, 80, 160]$, SNR $= [-0.8, -3.5, -5.2]$ dB and non-IID noise. (d) $M = 5$, $N = [40, 120, 200]$, SNR $= [-1.3, -4.2]$ dB and non-IID noise.

Gaussian distribution, which are fixed during the sensing period but change cross Monte Carlo runs. Without loss of generality, the channel is normalized as $\bar{\mathbf{h}}_i = \mathbf{h}_i/\|\mathbf{h}_i\|$, the noise variance is set to one for IID noise and the averaged noise variance is set to one for non-IID noise. In the sequel, the population covariance matrix under $\mathcal{H}_1$ is $\mathbf{R} = \mathbf{I}_M + \sum_{i=1}^{q} \sigma_{u_i} \bar{\mathbf{h}}_i \bar{\mathbf{h}}_i^{\mathrm{H}}$ for IID noise and $\mathbf{R} = \mathrm{diag}(\sigma_{n_1}, \ldots, \sigma_{n_M}) + \sum_{i=1}^{q} \sigma_{u_i} \bar{\mathbf{h}}_i \bar{\mathbf{h}}_i^{\mathrm{H}}$ for non-IID noise. The SNR corresponding to the i-th signal is defined as $\mathrm{SNR}_i = 10 \log_{10} \sigma_{u_i}$. For the NC primary signals, their noncircularity phases $\{\phi_i\}_{i=1}^{q}$ are drawn from a uniform distribution within $[-\pi, \pi)$ and their noncircularity rates are equal to one, i.e., $\kappa_1 = \cdots = \kappa_q = 1$. This situation corresponds to the BPSK or offset QPSK modulated signals [45], [46]. As a result, the true complementary covariance matrix is $\tilde{\mathbf{R}} = \sum_{i=1}^{q} \mathrm{SNR}_i e^{\iota \phi_i} \bar{\mathbf{h}}_i \bar{\mathbf{h}}_i^{\mathrm{T}}$.

It is seen in Fig. 2 that the proposed Beta approximation is vary accurate in terms of fitting the simulated detection probability. In particular, the errors between

the analytical and simulated detection probabilities are $[1.45, 1.04, 0.67] \times 10^{-5}$ in Fig. 2(a), $[0.99. 0.63, 0.49] \times 10^{-5}$ in Fig. 2(b), $[0.48, 0.43, 0.31] \times 10^{-5}$ in Fig. 2(c) and $[0.24, 0.21, 0.19] \times 10^{-5}$ in Fig. 2(d). Note that the errors are still computed by (51) where $F(y_i)$ and $\hat{F}(y_i)$ are replaced by $G(y_i)$ and $\hat{G}(y_i)$, which stand for the simulated and analytical detection probabilities, respectively. Thus, the derived Beta approximation is able to provide sufficiently precise prediction for the detection probability of the NC-HDM approach under IID and non-IID noises.

B. Detection Performance

In this subsection, we evaluate the robustness as well as accuracy of the NC-HDM detection algorithm for complex-valued noncircular primary signals by comparing its empirical ROCs with those of the state-of-the-art methods. In particular, the decision threshold is varied to calculate the false-alarm probability and its corresponding detection probability, leading to the ROC
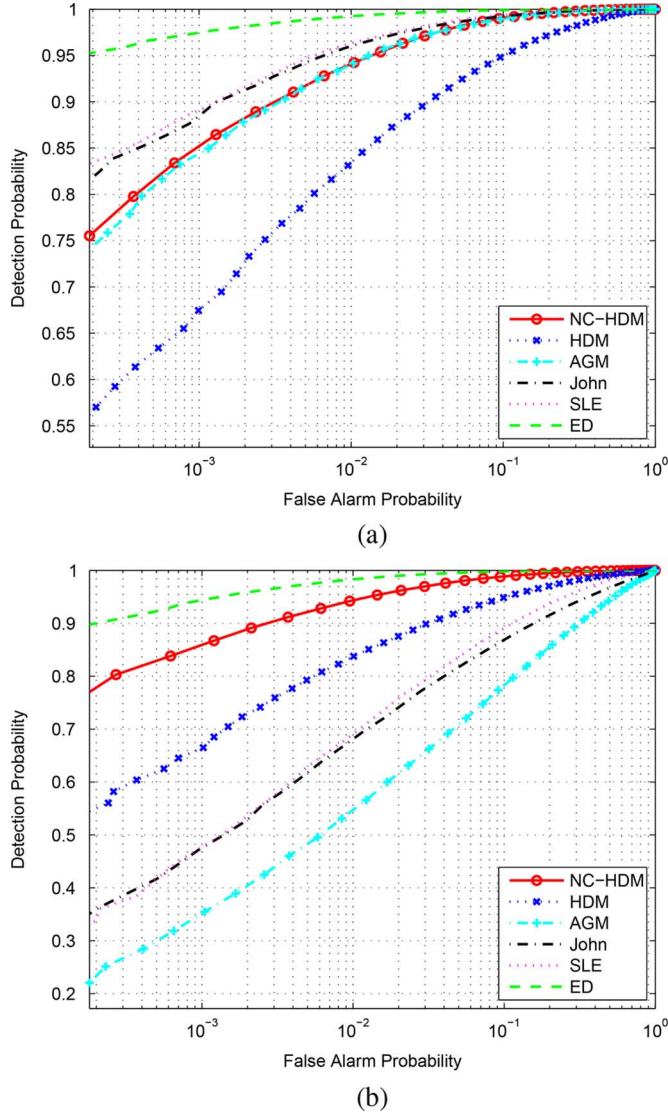
Fig. 3. ROCs of various detectors in Rayleigh fading channel. $M = 3$, $N = 30$, $q = 1$ and $\mathrm{SNR} = 4$ dB. (a) IID noise. (b) Non-IID noises with powers $[1.6, 0.9, -2.5]$ dB.

Fig. 4. ROCs of various detectors in Rayleigh fading channel. $M = 3$, $N = 30$, $q = 2$ and $\mathrm{SNR} = [4, 3]$ dB. (a) IID noise. (b) Non-IID noises with powers $[1.6, 0.9, -2.5]$ dB.

curve. For the purpose of comparison, the numerical results of the HDM, AGM, John's, SLE as well as ED algorithms are provided. As the true noise variance is unknown *a priori* to the receiver in practice, the ED approach is used herein as the benchmark. In addition, the Rayleigh fading channel model addressed above is employed. All the numerical results are obtained from 10^5 Monte Carlo trials.

The ROCs of the NC-HDM, HDM, AGM, John's, SLE and ED algorithms in Rayleigh fading channel are demonstrated in Fig. 3, where the number of antennas equals 3, the number of samples is 30 and the SNR equals 4 dB for a single primary signal. It is indicated in Fig. 3(a) that, for the situation of a single primary signal and small sample size, the NC-HDM approach is superior to the AGM and HDM methods but inferior to the SLE and John's detectors. This is because the SLE approach uses the *a priori* knowledge of the primary signal number, i.e., $q = 1$, while the other algorithms do not utilize this information. Moreover, recall that John's method is known to be the locally
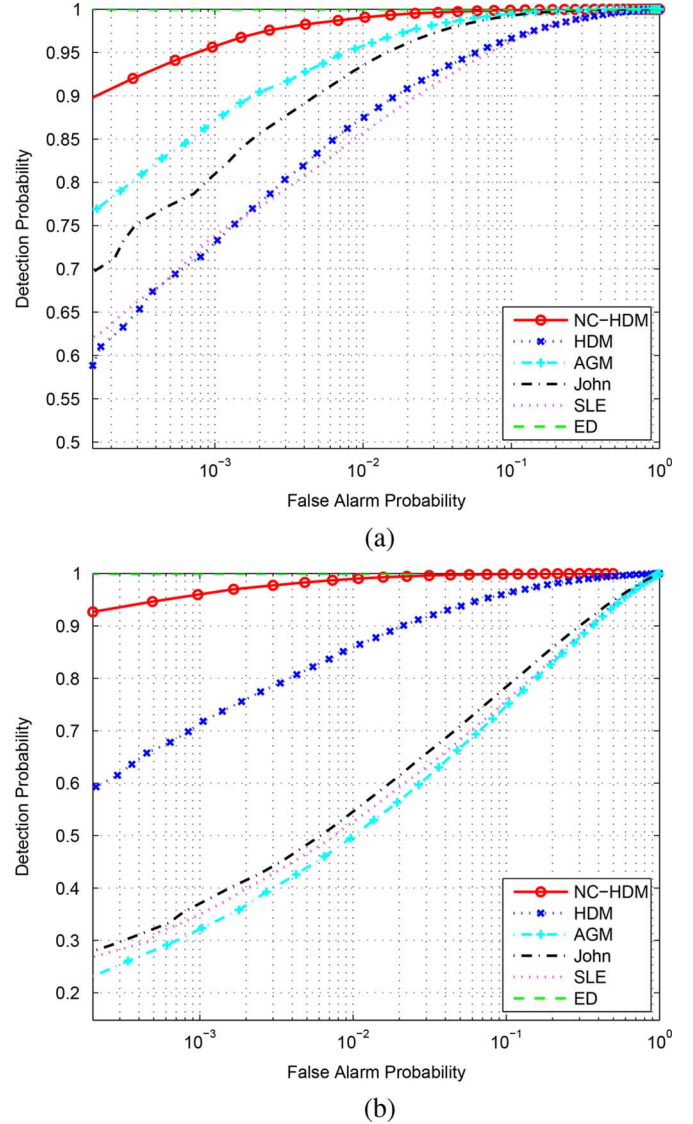
most powerful invariant test for sphericity. It is superior to the other schemes for small samples and single primary signal but not robust against the non-IID noise, as verified in Fig. 3(b). Instead, the NC-HDM approach significantly outperforms the other algorithms except the ED method, particularly for non-IID noise. Recall that the HDM algorithm is well known to be robust against the non-IID noise but fails to employ the property of the NC signals for spectrum sensing. This is why it is inferior to the NC-HDM approach.

The simulation results for two primary signals with powers [4,3] dB are plotted in Fig. 4 in which the other parameters are the same as those in Fig. 3. It is observed that the NC-HDM algorithm is considerably superior to the SLE, AGM, HDM and John's in terms of detection probability since it is able to efficiently utilize the NC property of the primary signals and considers the non-uniform noise powers. For the scenario of a single primary signal and large sample size, the numerical results are plotted in Fig. 5. It is seen that the NC-HDM detector
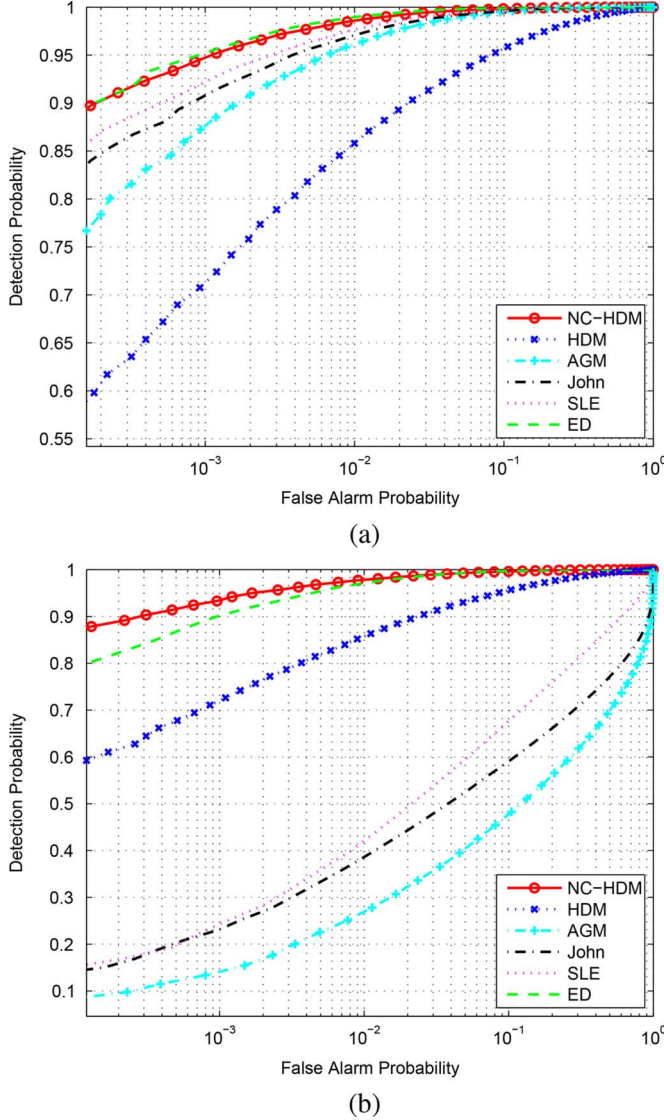
(a)

(b)

Fig. 5. ROCs of various detectors in Rayleigh fading channel. $M = 3$, $N = 100$, $q = 1$ and $\mathrm{SNR} = 0$ dB. (a) IID noise. (b) Non-IID noise with powers $[1.6, 0.9, -2.5]$ dB.

(a)

(b)

Fig. 6. ROCs of various detectors in Rayleigh fading channel. $M = 4$, $N = 100$, $q = 2$ and $\mathrm{SNR} = [-1, -2]$ dB. (a) IID noise. (b) Non-IID noise with powers $[2.3, 1.6, -1.7, -2.2]$ dB.

surpasses the SLE approach and ever is comparable with the ED scheme in detection performance for IID noise. Furthermore, the NC-HDM approach is capable of offering the best detection performance among all the studied schemes for non-IID noises, as illustrated in Fig. 5(b). The similar results are observed in Fig. 6, where the numbers of antennas is 4, the number of samples is 100, the number of primary signals equals 2 and the SNRs are set as $[-1, -2]$ dB. It is seen that although the ED approach is able to provide the optimal detection performance for IID noise, its detection performance considerably degrades for non-IID noise. This in turn means that the ED scheme is not robust against the non-IID noise. On the contrary, the NC-HDM test is robust against the non-IID noise because its derivation has removed the difference among the noise variances. On the other hand, the NC-HDM algorithm is able to employ the whole statistical property of the NC primary signals, namely, the usual covariance matrix and complementary covariance matrix, for
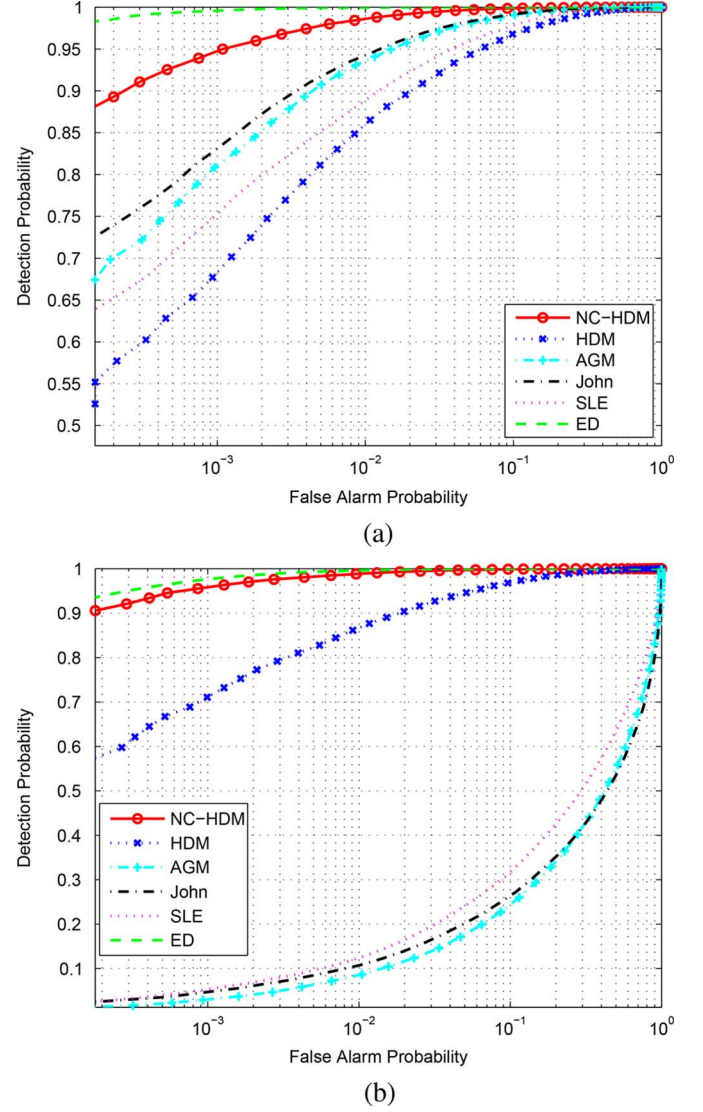
spectrum sensing while other approaches ignore the complementary covariance matrix. Hence, the NC-HDM approach surpasses the state-of-the-art methods in terms of accuracy and/or robustness.

VI. CONCLUSION

By means of exploiting the NC property of the primary signals and considering the non-uniform noise, a robust and accurate variant of the HDM test has been devised in this paper. Moreover, utilizing the asymptotic Box's approximation, the theoretical false-alarm probability has been derived, enabling us to accurately and analytically calculate the theoretical decision threshold for the proposed NC-HDM method in practical spectrum sensing. Furthermore, employing the asymptotic Beta approximation, we produce accurate and analytical formula for the detection probability of the NC-HDM approach. Extensive simulation results demonstrate the superiority of the NC-HDM algorithm and agree well with our theoretical computations.

APPENDIX A
PROOF OF PROPOSITION 1

It follows from (39) and (40) that the diagonal elements of $\underline{\mathbf{W}}'$, i.e., w'_{ii}, in (38) can be determined by the diagonal elements of $\mathbf{G}$ with DOFs of $N + k$. That is, $w'_{ii} = g_{ii} + g_{(i+M)(i+M)}$ for $1 \leq i \leq M$. As a result, we obtain

$$
\prod_{i=1}^{M} w'_{ii}
$$

$$
= \prod_{i=1}^{M} (g_{ii} + g_{(i+M)(i+M)})
$$

$$
= \sum_{\ell_1=0}^{1} \sum_{\ell_2=0}^{1} \cdots \sum_{\ell_M=0}^{1} g_{(1+\ell_1 M)(1+\ell_1 M)} g_{(2+\ell_2 M)(2+\ell_2 M)} \times \cdots
$$

$$
\times g_{(M+\ell_M M)(M+\ell_M M)}
$$

$$
\triangleq \sum_{\ell_1=0}^{1} \sum_{\ell_2=0}^{1} \cdots \sum_{\ell_M=0}^{1} g_{i_1 i_1} \cdots g_{i_M i_M} \qquad (52)
$$

with $i_m = m + \ell_m M (m = 1, \ldots, M)$ and [see (53) at the bottom of the page], with $j_{2m-1} = m + \ell_{2m-1} M (m = 1, \ldots, M)$ and $j_{2m} = m + \ell_{2m} M (m = 1, \ldots, M)$. To determine $E[\prod_{i=1}^{M} w'_{ii}]$, we need to calculate $E[g_{i_1 i_1} \cdots g_{i_M i_M}]$ for $\ell_m = 0$ or $\ell_m = 1$ with $m = 1, \ldots, M$. Similarly, the determination of $E[\prod_{i=1}^{2M} w'^2_{ii}]$ amounts to the computation of $E[g_{j_1 j_1} \cdots g_{j_{2M} j_{2M}}]$ for $\ell_m = 0$ or $\ell_m = 1$ with $m = 1, \ldots, 2M$. To this end, we need to use the following results ([39], pp.261).

Lemma 2: If $\mathbf{G} \sim \mathcal{W}_{2M}(N + k, \mathbf{\Sigma})$ with $\mathbf{\Sigma} = E[\check{\mathbf{x}} \check{\mathbf{x}}^{\mathrm{T}}] \triangleq (\sigma_{ij})_{2M \times 2M} \succ \mathbf{0}$ and there are collections $\mathbf{c} = \{i_1, \ldots, i_M\}$, $\mathbf{d} = \{i_{M+1}, \ldots, i_{2M}\}$ such that $\mathbf{c} \cap = \phi$ and $\mathbf{c} \cup \mathbf{d} = \{i_1, \ldots, i_{2M}\}$, then we have

$$
\begin{bmatrix} \mathbf{G}_{cc} & \mathbf{G}_{cd} \\ \mathbf{G}_{dc} & \mathbf{G}_{dd} \end{bmatrix} \sim \mathcal{W}_{2M} \left(N + k, \begin{bmatrix} \mathbf{\Sigma}_{cc} & \mathbf{\Sigma}_{cd} \\ \mathbf{\Sigma}_{dc} & \mathbf{\Sigma}_{dd} \end{bmatrix} \right) \qquad (54)
$$

where $\mathbf{G}_{cd}$ is the $M \times M$ matrix consisting of the elements of $\mathbf{G}$ with indices $\mathbf{c}$ and $\mathbf{d}$ while $\mathbf{\Sigma}_{cd}$ is the $M \times M$ matrix consisting of the elements of $\mathbf{\Sigma}$ with indices $\mathbf{c}$ and $\mathbf{d}$. This definition is valid for other matrices in (54).

As a result, we can determine $E[\prod_{i=1}^{M} w'_i]$ by means of the distribution of $\mathbf{G}_{cc}$. It follows from Lemma 2 that $\mathbf{G}_{cc}$ follows a real Wishart distribution, i.e., $\mathbf{G}_{cc} \sim \mathcal{W}_M(N + k, \mathbf{\Sigma}_{cc})$. Accordingly, it follows from ([47], (5.12)) that the characteristic function is

$$
\phi(\mathbf{\Theta}_{cc}) = |\mathbf{I}_M - 2\imath \mathbf{\Theta}_{cc} \mathbf{\Sigma}_{cc}|^{-\frac{N+k}{2}} \qquad (55)
$$

where $\mathbf{\Theta}_{cc}$ is the matrix argument of the characteristic function. In order to obtain the characteristic function of the diagonal elements of $\mathbf{G}_{cc}$, namely, the collection composed of any M elements of $\{g_{11}, \ldots, g_{MM}, g_{(1+M)(1+M)}, \ldots, g_{(2M)(2M)}\}$, we replace $\mathbf{\Theta}_{cc}$ in (55) with $\mathbf{D}_{cc} \triangleq \mathrm{diag}(t_{i_1}, \ldots, t_{i_M})$, yielding the characteristic function (56), shown at the bottom of the page. As a result, we have

$$
E[g_{i_1 i_1} \cdots g_{i_M i_M}] = \frac{1}{\imath^M} \frac{\partial^M \phi(t_{i_1}, \ldots, t_{i_M})}{\partial t_{i_1} \cdots \partial t_{i_M}} \Bigg|_{\mathbf{D}_{cc}=\mathbf{0}}
$$

$$
= \frac{1}{\imath^M} \frac{\partial^M |\mathbf{A}_{cc}|^{-\frac{N+1}{2}}}{\partial t_{i_1} \cdots \partial t_{i_M}} \Bigg|_{\mathbf{D}_{cc}=\mathbf{0}} . \qquad (57)
$$

The partial derivatives of $|\mathbf{A}_{cc}|^{-\frac{N+1}{2}}$ with respect to $t_{i_1}, \ldots, t_{i_M}$ are given as

$$
\frac{\partial^M |\mathbf{A}_{cc}|^{-\frac{N+1}{2}}}{\partial t_{i_1} \cdots \partial t_{i_M}} = \sum_{\boldsymbol{\pi} \in \mathcal{S}_M} \left[\prod_{m=1}^{p^{(\boldsymbol{\pi})}} (N + 2m - 1) \right] |\mathbf{A}_{cc}|^{-\frac{N+1}{2} - p^{(\boldsymbol{\pi})}}
$$

$$
\times \left(-\frac{1}{2} \right)^{p^{(\boldsymbol{\pi})}} \prod_{m=1}^{p^{(\boldsymbol{\pi})}} \frac{\partial^{J} |\mathbf{A}_{cc}|}{\partial \pi_{m1} \cdots \partial \pi_{mJ}} \qquad (58)
$$

$$
\prod_{i=1}^{M} w'^2_{ii} = \sum_{\ell_1=0}^{1} \sum_{\ell_2=0}^{1} \cdots \sum_{\ell_{2M}=0}^{1} g_{(1+\ell_1 M)(1+\ell_1 M)} g_{(1+\ell_2 M)(1+\ell_2 M)}
$$

$$
\times g_{(2+\ell_3 M)(2+\ell_3 M)} g_{(2+\ell_4 M)(2+\ell_4 M)} \times \cdots
$$

$$
\times g_{(M+\ell_{2M-1} M)(M+\ell_{2M-1} M)} g_{(M+\ell_{2M} M)(M+\ell_{2M} M)}
$$

$$
\triangleq \sum_{\ell_1=0}^{1} \sum_{\ell_2=0}^{1} \cdots \sum_{\ell_{2M}=0}^{1} g_{j_1 j_1} \cdots g_{j_{2M} j_{2M}} \qquad (53)
$$

$$
\phi(t_{i_1}, \ldots, t_{i_M}) = |\mathbf{I}_M - 2\imath \mathbf{D}_{cc} \mathbf{\Sigma}_{cc}|^{-\frac{N+k}{2}}
$$

$$
= \begin{vmatrix} 1 - 2\imath t_{i_1} \sigma_{i_1 i_1} & -2\imath t_{i_1} \sigma_{i_1 i_2} & \cdots & -2\imath t_{i_1} \sigma_{i_1 i_M} \\ -2\imath t_{i_2} \sigma_{i_2 i_1} & 1 - 2\imath t_{i_2} \sigma_{i_2 i_2} & \cdots & -2\imath t_{i_2} \sigma_{i_2 i_M} \\ \vdots & \vdots & \ddots & \vdots \\ -2\imath t_{i_M} \sigma_{i_M i_1} & -2\imath t_{i_M} \sigma_{i_M i_2} & \cdots & 1 - 2\imath t_{i_M} \sigma_{i_M i_M} \end{vmatrix}^{-\frac{N+k}{2}}
$$

$$
\triangleq |\mathbf{A}_{cc}|^{-\frac{N+k}{2}} . \qquad (56)
$$

where $\mathcal{S}_M$, $\boldsymbol{\pi}$, $p^{(\boldsymbol{\pi})}$, $\boldsymbol{\pi}_m$, π_{mj} and j are defined in Proposition 1. To illustrate the partition $\boldsymbol{\pi}$, we consider an example of 3-element set $\{t_1, t_2, t_3\}$, which provides five different partitions. That is,

$$\boldsymbol{\pi} = \{\boldsymbol{\pi}_1, \boldsymbol{\pi}_2, \boldsymbol{\pi}_3\}, \boldsymbol{\pi}_1 = \{t_1\}, \boldsymbol{\pi}_2 = \{t_2\}, \boldsymbol{\pi}_3 = \{t_3\}, p^{(\boldsymbol{\pi})} = 3 \tag{59a}$$

$$\boldsymbol{\pi} = \{\boldsymbol{\pi}_1, \boldsymbol{\pi}_2\}, \boldsymbol{\pi}_1 = \{t_1\}, \boldsymbol{\pi}_2 = \{t_2, t_3\}, p^{(\boldsymbol{\pi})} = 2 \tag{59b}$$

$$\boldsymbol{\pi} = \{\boldsymbol{\pi}_1, \boldsymbol{\pi}_2\}, \boldsymbol{\pi}_1 = \{t_1, t_2\}, \boldsymbol{\pi}_2 = \{t_3\}, p^{(\boldsymbol{\pi})} = 2 \tag{59c}$$

$$\boldsymbol{\pi} = \{\boldsymbol{\pi}_1, \boldsymbol{\pi}_2\}, \boldsymbol{\pi}_1 = \{t_1, t_3\}, \boldsymbol{\pi}_2 = \{t_2\}, p^{(\boldsymbol{\pi})} = 2 \tag{59d}$$

$$\boldsymbol{\pi} = \{\boldsymbol{\pi}_1\}, \boldsymbol{\pi}_1 = \{t_1, t_2, t_3\}, p^{(\boldsymbol{\pi})} = 1. \tag{59e}$$

For the last partition in (59e), we have $\pi_{11} = t_1, \pi_{12} = t_2, \pi_{13} = t_3$ and $j = 3$.

Noticing that

$$|\mathbf{A}_{cc}||_{\mathbf{D}_{cc}=\mathbf{0}} = 1 \tag{60}$$

and substituting (58) into (57), we have

$$E[g_{i_1 i_1} \cdots g_{i_M i_M}] = \frac{1}{i^M} \sum_{\boldsymbol{\pi} \in \mathcal{S}_M} \left[\prod_{m=1}^{p^{(\boldsymbol{\pi})}} (N + 2m - 1) \right] \left(-\frac{1}{2} \right)^{p^{(\boldsymbol{\pi})}}$$

$$\times \prod_{m=1}^{p^{(\boldsymbol{\pi})}} \frac{\partial^j |\mathbf{A}_{cc}|}{\partial \pi_{m1} \cdots \partial \pi_{mj}} \Bigg|_{\mathbf{D}_{cc}=\mathbf{0}}. \tag{61}$$

Therefore, it follows from (52) and (61) that $E[\prod_{i=1}^M w'_{ii}]$ can be eventually expressed as (41). On the other hand, the partial derivatives of $|\mathbf{A}_{cc}|$ with respect to the elements of $\boldsymbol{\pi}$, i.e., $t_{i_m}(m = 1, \ldots, M)$, are computed as (62), shown at the bottom of the page.

In order to determine $E[\prod_{i=1}^M w'^2_{ii}]$, we need to use the whole SCM $\mathbf{G}$, whose characteristic function is given as

$$\varphi(\boldsymbol{\Theta}) = |\mathbf{I}_{2M} - 2i\boldsymbol{\Theta}\boldsymbol{\Sigma}|^{-\frac{N+k}{2}} \tag{63}$$

where $\boldsymbol{\Theta}$ is the matrix argument of the characteristic function. To compute the characteristic function of $g_{j_1 j_1}, \ldots, g_{j_{2M} j_{2M}}$, we replace $\boldsymbol{\Theta}$ in (63) with $\mathbf{D}_{2M} \triangleq \text{diag}(t_1, \ldots, t_{2M})$, yielding the characteristic function (64), given at the bottom of the page. As a result, we have

$$E[g_{j_1 j_1} \cdots g_{j_{2M} j_{2M}}] = \frac{1}{i^{2M}} \frac{\partial^{2M} \varphi(t_1, \ldots, t_{2M})}{\partial t_{j_1} \cdots \partial t_{j_{2M}}} \Bigg|_{\mathbf{D}_{2M}=\mathbf{0}}$$

$$= \frac{1}{i^{2M}} \frac{\partial^{2M} |\mathbf{A}_{2M}|^{-\frac{N+2}{2}}}{\partial t_{j_1} \cdots \partial t_{j_{2M}}} \Bigg|_{\mathbf{D}_{2M}=\mathbf{0}}. \tag{65}$$

$$\frac{\partial |\mathbf{A}_{cc}|}{\partial t_{i_1}} \Bigg|_{t_{i_1}=0} = \begin{vmatrix} -i2\sigma_{i_1 i_1} & -i2\sigma_{i_1 i_2} & \cdots & -i2\sigma_{i_1 i_M} \\ 0 & 1 & \cdots & 0 \\ \vdots & \vdots & \ddots & \vdots \\ 0 & 0 & \cdots & 1 \end{vmatrix}$$

$$= -i2\sigma_{i_1 i_1} \tag{62a}$$

$$\frac{\partial^2 |\mathbf{A}_{cc}|}{\partial t_{i_1} \partial t_{i_2}} \Bigg|_{\substack{t_{i_1}=0 \\ t_{i_2}=0}} = \begin{vmatrix} -i2\sigma_{i_1 i_1} & -i2\sigma_{i_1 i_2} & -i2\sigma_{i_1 i_3} & \cdots & -i2\sigma_{i_1 i_M} \\ -i2\sigma_{i_2 i_1} & -i2\sigma_{i_2 i_2} & -i2\sigma_{i_2 i_3} & \cdots & -i2\sigma_{i_2 i_M} \\ 0 & 0 & 1 & \cdots & 0 \\ \vdots & \vdots & \vdots & \ddots & \vdots \\ 0 & 0 & 0 & \cdots & 1 \end{vmatrix}$$

$$= (-i2)^2 \begin{vmatrix} \sigma_{i_1 i_1} & \sigma_{i_1 i_2} \\ \sigma_{i_2 i_1} & \sigma_{i_2 i_2} \end{vmatrix}$$

$$\vdots \tag{62b}$$

$$\frac{\partial^M |\mathbf{A}_{cc}|}{\partial t_{i_1} \cdots \partial t_{i_M}} \Bigg|_{\mathbf{D}_{cc}=\mathbf{0}} = (-2i)^M |\boldsymbol{\Sigma}_{cc}|. \tag{62c}$$

$$\varphi(t_1, \ldots, t_{2M}) = |\mathbf{I}_{2M} - 2i\mathbf{D}_{2M}\boldsymbol{\Sigma}|^{-\frac{N+k}{2}}$$

$$= \begin{vmatrix} 1 - 2it_1\sigma_{11} & -2it_1\sigma_{12} & \cdots & -2it_1\sigma_{1(2M)} \\ -2it_2\sigma_{21} & 1 - 2it_2\sigma_{22} & \cdots & -2it_2\sigma_{2(2M)} \\ \vdots & \vdots & \ddots & \vdots \\ -2it_{2M}\sigma_{(2M)1} & -2it_{2M}\sigma_{(2M)2} & \cdots & -2it_{2M}\sigma_{(2M)(2M)} \end{vmatrix}^{-\frac{N+k}{2}}$$

$$\triangleq |\mathbf{A}_{2M}|^{-\frac{N+k}{2}}. \tag{64}$$

Similar to (58), let $\mathcal{S}_{2M}$ be composed of all the partitions of the $2M$-element set $\{t_{j_1}, \ldots, t_{j_{2M}}\}^2$. Meanwhile, note that the second-order partial derivatives of $|\mathbf{A}_{2M}|$ with respect to the same variable t_{j_m} are equal to zero. Consequently, the partial derivatives of $|\mathbf{A}_{2M}|^{-\frac{N+2}{2}}$ with respect to $t_{j_1}, \ldots, t_{j_{2M}}$ are given as

$$\frac{\partial^{2M}|\mathbf{A}_{2M}|^{-\frac{N+2}{2}}}{\partial t_{j_1} \cdots \partial t_{j_{2M}}} = \sum_{\boldsymbol{\pi} \in \mathcal{S}_{2M}} \left[\prod_{m=1}^{p^{(\boldsymbol{\pi})}} (N+2m) \right] |\mathbf{A}_{2M}|^{-\frac{N+2}{2}-p^{(\boldsymbol{\pi})}}$$
$$\times \left(-\frac{1}{2}\right)^{p^{(\boldsymbol{\pi})}} \prod_{m=1}^{p^{(\boldsymbol{\pi})}} \frac{\partial^{j}|\mathbf{A}_{2M}|}{\partial \pi_{m1} \cdots \partial \pi_{mJ}}. \quad (66)$$

Hence, substituting

$$|\mathbf{A}_{2M}|_{\mathbf{D}_{2M}=\mathbf{0}} = 1 \quad (67)$$

along with (66) into (65), it follows from (53) that $E[\prod_{i=1}^{M} w_{ii}'^2]$ can be calculated as (42). Recall that, for $\ell_{2m-1} = \ell_{2m}(m = 1, \ldots, M)$, we have $t_{j_{2m-1}} = t_{j_{2m}}$. In such a situation, the partial derivatives of $|\mathbf{A}_{2M}|$ are equal to zero. In other words, the second-order partial derivatives of $|\mathbf{A}_{2M}|$ with respect to the same variable t_{j_m} in (66) are zero. On the other hand, for the scenario where $\boldsymbol{\pi}$ contains different variables, i.e., $t_i \neq t_j(i, j = 1, \ldots, 2M)$, we can utilize the same manipulation as (62) to obtain the partial derivatives of $|\mathbf{A}_{2M}|$ with respect to the elements of $\boldsymbol{\pi}$, i.e., $t_i(i = 1, \ldots, 2M)$. That is

$$\left.\frac{\partial|\mathbf{A}_{2M}|}{\partial t_1}\right|_{t_1=0} = -\imath 2\sigma_{11} \quad (68\text{a})$$

$$\left.\frac{\partial^2|\mathbf{A}_{2M}|}{\partial t_1 \partial t_2}\right|_{\substack{t_1=0 \\ t_2=0}} = (-\imath 2)^2 \begin{vmatrix} \sigma_{11} & \sigma_{12} \\ \sigma_{21} & \sigma_{22} \end{vmatrix}$$

$$\vdots \quad (68\text{b})$$

$$\left.\frac{\partial^{2M}|\mathbf{A}_{2M}|}{\partial t_1 \cdots \partial t_{2M}}\right|_{\mathbf{D}_{2M}=\mathbf{0}} = (-2\imath)^{2M}|\boldsymbol{\Sigma}_{2M}|. \quad (68\text{c})$$

This completes the proof of Proposition 1.

REFERENCES

[1] J. Mitola, III, "Cognitive radio for flexible mobile multimedia communications," in *Proc. IEEE Int. Workshop on Mobile Multimedia Commun. (MoMuC)*, San Diego, CA, Nov. 1999, pp. 3–10.

[2] S. Haykin, "Cognitive radio: Brain-empowered wireless communications," *IEEE J. Sel. Areas Commun.*, vol. 23, no. 2, pp. 201–220, Feb. 2005.

[3] E. Axell, G. Leus, E. G. Larsson, and H. V. Poor, "Spectrum sensing for cognitive radio: State-of-the-art and recent advances," *IEEE Signal Process. Mag.*, vol. 29, no. 3, May 2012.

[4] H. Urkowitz, "Energy detection of unknown deterministic signals," *Proc. IEEE*, vol. 55, no. 4, pp. 523–531, Apr. 1967.

[5] F. F. Digham, M. S. Alouini, and M. K. Simon, "On the energy detection of unknown signals over fading channels," *IEEE Trans. Comput.*, vol. 55, no. 1, pp. 21–24, Jan. 2007.

[6] V. Koivunen, S. Chaudhari, and H. V. Poor, "Autocorrelation-based decentralized sequential detection of OFDM signals in cognitive radios," *IEEE Trans. Signal Process.*, vol. 57, no. 7, pp. 2690–2700, Jul. 2009.

[7] A. Huttunen, J. Lundén, V. Koivunen, and H. V. Poor, "Spectrum sensing in cognitive radios based on multiple cyclic frequencies," in *Proc. 2nd Int. Conf. Cogn. Radio Oriented Wireless Netw. Commun.*, Orlando, FL, Aug. 2007, pp. 37–43.

[8] A. Huttunen, J. Lundén, V. Koivunen, and H. V. Poor, "Collaborative cyclostationary spectrum sensing for cognitive radio systems," *IEEE Trans. Signal Process.*, vol. 57, no. 11, pp. 4182–4195, Nov. 2009.

[9] Y. Zeng, C. L. Koh, and Y.-C. Liang, "Maximum eigenvalue detection: Theory and application," in *Proc. IEEE Int. Conf. Commun. (ICC)*, Beijing, China, May 2008, pp. 4160–4164.

[10] A. Kortun, T. Ratnarajah, M. Sellathurai, C. Zhong, and C. B. Papadias, "On the performance of eigenvalue-based cooperative spectrum sensing for cognitive radio," *IEEE J. Sel. Topics Signal Process*, vol. 5, no. 1, pp. 49–55, Feb. 2011.

[11] Q. T. Zhang, "Theoretical performance and thresholds of the multitaper method for spectrum sensing," *IEEE Trans. Veh. Technol.*, vol. 60, no. 5, pp. 2128–2138, Jun. 2011.

[12] L. Wei, P. Dharmawansa, and O. Tirkkonen, "Multiple primary user spectrum sensing in the low SNR regime," *IEEE Trans. Commun.*, vol. 61, no. 5, pp. 1720–1731, May 2013.

[13] L. Wei and O. Tirkkonen, "Spectrum sensing in the presence of multiple primary users," *IEEE Trans. Commun.*, vol. 60, no. 5, pp. 1268–1277, 2012.

[14] S. K. Sharma, S. Chatzinotas, and B. Ottersten, "Eigenvalue based sensing and SNR estimation for cognitive radio in presence of noise correlation," *IEEE Trans. Veh. Technol.*, vol. 62, no. 8, pp. 3671–3684, Aug. 2013.

[15] R. Zhang, T. J. Lim, Y.-C. Liang, and Y. Zeng, "Multi-antenna based spectrum sensing for cognitive radios: A GLRT approach," *IEEE Trans. Commun.*, vol. 58, no. 1, pp. 84–88, Jan. 2010.

[16] T. J. Lim, R. Zhang, Y. C. Liang, and Y. H. Zeng, "GLRT-based spectrum sensing for cognitive radio," in *Proc. IEEE Global Telecommun. Conf. (GLOBECOM 08)*, New Orleans, LA, USA, Dec. 2008, pp. 1–5.

[17] O. Ledoit and M. Wolf, "Some hypothesis tests for the covariance matrix when the dimension is large compared to the sample size," *Ann. Statist.*, vol. 30, no. 4, pp. 1081–1102, 2002.

[18] S. John, "Some optimal multivariate tests," *Biometrika*, vol. 58, no. 1, pp. 123–127, Apr. 1971.

[19] J. K. Tugnait, "On multiple antenna spectrum sensing under noise variance uncertainty and flat fading," *IEEE Trans. Signal Process.*, vol. 60, no. 4, pp. 1823–1832, Apr. 2012.

[20] A. Mariani, A. Giorgetti, and M. Chiani, "Test of independence for cooperative spectrum sensing with uncalibrated receivers," in *Proc. IEEE Global Commun. Conf. (GLOBECOM)*, Anaheim, CA, Dec. 2012, pp. 1374–1379.

[21] D. Ramírez, G. Vazquez-Vilar, R. López-Valcarce, J. Vía, and I. Santamaría, "Detection of rank-p signals in cognitive radio networks with uncalibrated multiple antennas," *IEEE Trans. Signal Process*, vol. 59, no. 8, pp. 3764–3774, Aug. 2011.

[22] R. López-Valcarce, G. Vazquez-Vilar, and J. Sala, "Multiantenna spectrum sensing for cognitive radio: Overcoming noise uncertainty," in *Proc. IEEE Int. Workshop on Cogn. Inf. Process. (CIP)*, Elba Island, Italy, Jun. 2010, pp. 310–315.

[23] R. Li, L. Huang, Y. Shi, and H. C. So, "Gerschgorin disk-based robust spectrum sensing for cognitive radio," in *Proc. IEEE Int. Conf. Acoust., Speech, Signal Process. (ICASSP'14)*, Florence, Italy, May 2014, pp. 1–4.

[24] J. Vía, D. Ramírez, and I. Santamaría, "The locally most powerful test for multiantenna spectrum sensing with uncalibrated receivers," in *Proc. IEEE Int. Conf. Acoust., Speech Signal Process. (ICASSP)*, Kyoto, Japan, Mar. 2012, pp. 3437–3440.

[25] D. Ramírez, J. Vía, I. Santamaría, and L. L. Scharf, "Locally most powerful invariant tests for correlation and sphericity of Gaussian vectors," *IEEE Trans. Inf. Theory*, vol. 59, no. 4, Apr. 2013.

[26] L. Huang, H. C. So, and C. Qiang, "Volume-based method for spectrum sensing," *Digit. Signal Process.*, vol. 28, pp. 48–56, May 2014.

[27] L. Huang, C. Qian, Y. Xiao, and Q. T. Zhang, "Performance analysis of volume-based spectrum sensing for cognitive radio," pp. 1–14, Aug. 2014, DOI: 10.1109/TWC.2014.2345660.

---

^{2}According the definition of the index $j_m(m = 1, \ldots, 2M)$, we have $j_{2m-1} = j_{2m}$ for $\ell_{2m-1} = \ell_{2m}(m = 1, \ldots, M)$. Under such a condition, $t_{j_{2m-1}}$ and $t_{j_{2m}}$ are still taken as different variables in the partitions but the same variable in the derivatives.

[28] Y. Xu, Q. Wu, J. Wang, L. Shen, and A. Anpalagan, "Robust multiuser sequential channel sensing and access in dynamic cognitive radio networks: Potential games and stochastic learning," *IEEE Trans. Veh. Technol.*, pp. 1–14, 2014, DOI: 10.1109/TVT.2014.2356554, to be published.

[29] S. Wilks, "On the independence of k sets of normally distributed statistical variables," *Econometrica*, vol. 3, pp. 309–325, 1935.

[30] A. Leshem and A.-J. van der Veen, "Multichannel detection of Gaussian signals with uncalibrated receivers," *IEEE Signal Process. Lett.*, vol. 8, no. 4, pp. 120–122, Apr. 2001.

[31] A. Leshem and A.-J. van der Veen, "Multichannel detection and spatial signature estimation with uncalibrated receivers," in *Proc. 11th IEEE Workshop Stat. Signal Process.*, Singapore, Dec. 2001, pp. 190–193.

[32] S. Buzzi, M. Lops, and A. M. Tulino, "A new family of MMSE multiuser receivers for interference suppression in DS/CDMA systems employing BPSK modulation," *IEEE Trans. Comput.*, vol. 49, no. 1, pp. 154–167, Jan. 2001.

[33] A. Mirbagheri, N. Plataniotis, and S. Pasupathy, "An enhanced widely linear CDMA receiver with OQPSK modulation," *IEEE Trans. Comput.*, vol. 54, no. 2, pp. 261–272, Feb. 2006.

[34] P. Chevalier and F. Pipon, "New insights into optimal widely linear array receivers for the demodulation of BPSK, MSK, and GMSK interferencesł application to SAIC," *IEEE Trans. Signal Process*, vol. 54, no. 3, pp. 870–883, Mar. 2006.

[35] X.-L. Li, T. Adali, and M. Anderson, "Noncircular principal component analysis and its application to model selection," *Proc. IEEE*, vol. 59, no. 10, pp. 4516–4528, Oct. 2011.

[36] T. Adali, P. J. Schreier, and L. L. Scharf, "Complex-valued signal processing: The proper way to deal with impropriety," *Proc. IEEE*, vol. 59, no. 11, pp. 5101–5125, Nov. 2011.

[37] P. J. Schreier and L. L. Scharf, "Second-order analysis of improper complex random vectors and processes," *IEEE Trans. Signal Process.*, vol. 51, no. 3, pp. 714–725, Mar. 2003.

[38] G. E. P. Box, "A general distribution theory for a class of likelihood criteria," *Biometrika*, vol. 36, pp. 317–346, 1949.

[39] T. W. Anderson*, An Introduction to Multivariate Statistical Analysis*. New York: Wiley, 1984.

[40] R. A. Horn and C. R. Johnson*, Matrix Analysis*. Cambridge, U.K.: Cambridge Univ. Press, 1985.

[41] T. W. Anderson, "On the distribution of the two-sample Cramér-Von mises criterion," *Ann. Math. Statist.*, vol. 33, no. 3, pp. 1148–1159, 1962.

[42] L. Wei, O. Tirkkonen, P. Dharmawansa, and M. McKay, "On the exact distribution of the scaled largest eigenvalue," in *Proc. IEEE Int. Conf. Commun. (ICC)*, Ottawa, ON, Canada, Jun. 2012, pp. 2422–2426.

[43] A. T. Walden and P. Rubin-Delanchy, "On testing for impropriety of complex-valued Gaussian vectors," *Proc. IEEE*, vol. 57, no. 3, pp. 825–834, Mar. 2009.

[44] G. Rota, "The number of partitions of a set," *Amer. Math.*, vol. 71, pp. 498–504, 1964.

[45] M. Haardt and F. Römer, "Enhancements of unitary ESPRIT for noncircular sources," in *Proc. Int. Conf. Acoustics, Speech, Signal Processing (ICASSP)*, Montreal, QC, Canada, May 2004, vol. 2, pp. 101–104.

[46] H. Abeida and J.-P. Delmas, "MUSIC-like estimation of direction of arrival for noncircular sources," *Proc. IEEE*, vol. 54, no. 7, pp. 2678–2690, Jul. 2006.

[47] N. R. Goodman, "Statistical analysis based on a certain multivariate complex Gaussian distribution (An introduction)," *Ann. Math. Stat.*, vol. 34, pp. 152–177, 1963.

Lei Huang (M'07–SM'14) was born in Guangdong, China. He received the B.Sc., M.Sc., and Ph.D. degrees in electronic engineering from Xidian University, Xian, China, in 2000, 2003, and 2005, respectively.

From 2005 to 2006, he was a Research Associate with the Department of Electrical and Computer Engineering, Duke University, Durham, NC. From 2009 to 2010, he was a Research Fellow with the Department of Electronic Engineering, City University of Hong Kong, and a Research Associate with the Department of Electronic Engineering, The Chinese University of Hong Kong. From 2011 to 2014, he was a Professor with the Department of Electronic and Information Engineering, Harbin Institute of Technology Shenzhen Graduate School. Since November 2014, he has been with the College of Information Engineering, Shenzhen University, where he is currently a Chair Professor. His research interests include spectral estimation, array signal processing, statistical signal processing, and their applications in radar and wireless communication systems.

Dr. Huang is currently an editorial board member of *Digital Signal Processing*.
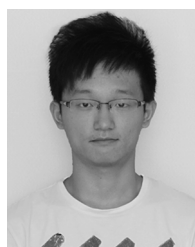
Yu-Hang Xiao was born in Anhui on January 20, 1992. He received the B.E. degree from Harbin Engineering University, Harbin, China, in 2012.

He is currently pursuing the Ph.D. degree in the field of communication and information engineering at HIT. His research interests are in statistical signal processing and spectrum sensing.

Q. T. Zhang (S'84–M'85–SM'95–F'09) received the B.Eng. degree from Tsinghua University, Beijing, and the M.Eng. degree from South China University of Technology, Guangzhou, China, both in wireless communications, and the Ph.D. degree in electrical engineering from McMaster University, Hamilton, Ontario, Canada.

He then joined McMaster University as a Researcher and Adjunct Assistant Professorship in 1986. In January 1992, he joined the Spar Aerospace Ltd., Satellite and Communication Systems Division, Montreal, as a Senior Member of Technical Staff. At Spar Aerospace, he participated in the development and manufacturing of the Radar Satellite (Radarsat). He joined Ryerson University, Toronto in 1993 and became a Professor in 1999. In 1999, he took one-year sabbatical leave at the National University of Singapore, and was a Chair Professor of Information Engineering at the City University of Hong Kong. His research interest is on wireless communications with current focus on wireless MIMO, cooperative systems, and cognitive radio.

Dr. Zhang served as an Associate Editor for the IEEE COMMUNICATIONS LETTERS from 2000 to 2007.